

RESEARCH

Open Access



Evaluating sex-specific responses to western diet across the lifespan: impact on cardiac function and transcriptomic signatures in C57BL/6J mice at 530 and 640/750 days of age

Ani Stepanyan^{1*†}, Agnieszka Brojakowska^{2,3†}, Roksana Zakharyan¹, Siras Hakobyan¹, Suren Davitavyan¹, Tamara Sirunyan¹, Gisane Khachatryan¹, Mary K. Khlgatian², Malik Bissier⁴, Shihong Zhang², Susmita Sahoo², Lahouaria Hadri⁵, Amit Rai⁶, Venkata Naga Srikanth Garikipati⁶, Arsen Arakelyan¹ and David A. Goukassian^{2*}

Abstract

Background Long-term consumption of Western Diet (WD) is a well-established risk factor for the development of cardiovascular disease (CVD); however, there is a paucity of studies on the long-term effects of WD on the pathophysiology of CVD and sex-specific responses.

Methods Our study aimed to investigate the sex-specific pathophysiological changes in left ventricular (LV) function using transthoracic echocardiography (ECHO) and LV tissue transcriptomics in WD-fed C57BL/6 J mice for 125 days, starting at the age of 300 through 425 days.

Results In female mice, consumption of the WD diet showed long-term effects on LV structure and possible development of HFpEF-like phenotype with compensatory cardiac structural changes later in life. In male mice, ECHO revealed the development of an HFrEF-like phenotype later in life without detectable structural alterations. The transcriptomic profile revealed a sex-associated dichotomy in LV structure and function. Specifically, at 530-day, WD-fed male mice exhibited differentially expressed genes (DEGs), which were overrepresented in pathways associated with endocrine function, signal transduction, and cardiomyopathies. At 750 days, WD-fed male mice exhibited dysregulation of several genes involved in various lipid, glucagon, and glutathione metabolic pathways. At 530 days, WD-fed female mice exhibited the most distinctive set of DEGs with an abundance of genes related to

[†]Ani Stepanyan and Agnieszka Brojakowska contributed equally to this work.

*Correspondence:

Ani Stepanyan
a_stepanyan@mb.sci.am
David A. Goukassian
david.goukassian@mssm.edu

Full list of author information is available at the end of the article



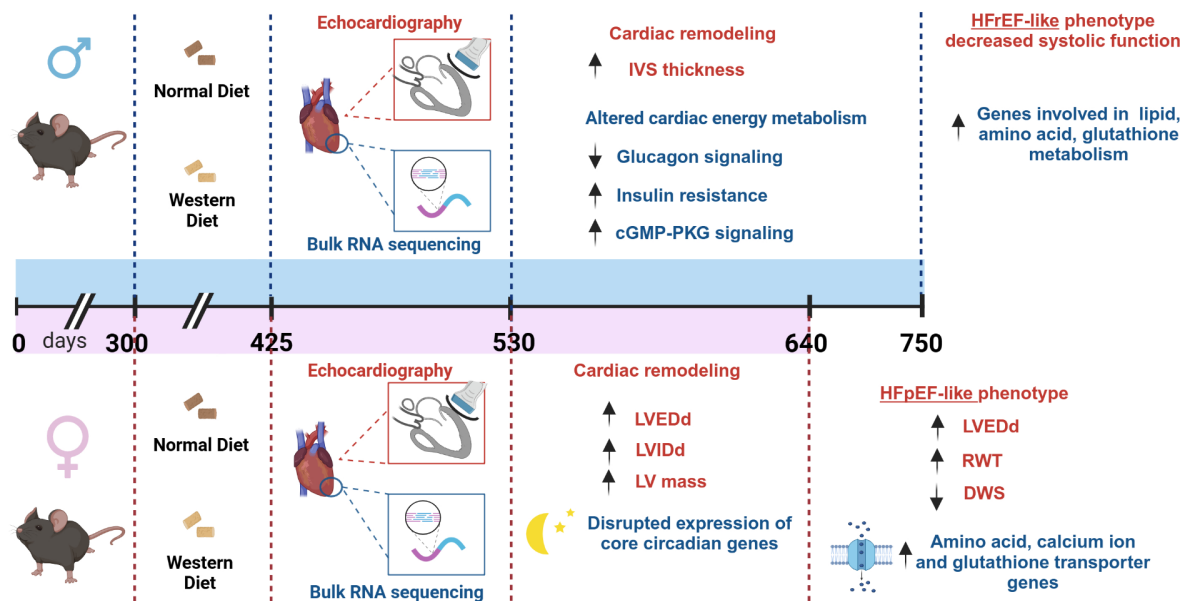
© The Author(s) 2024. **Open Access** This article is licensed under a Creative Commons Attribution-NonCommercial-NoDerivatives 4.0 International License, which permits any non-commercial use, sharing, distribution and reproduction in any medium or format, as long as you give appropriate credit to the original author(s) and the source, provide a link to the Creative Commons licence, and indicate if you modified the licensed material. You do not have permission under this licence to share adapted material derived from this article or parts of it. The images or other third party material in this article are included in the article's Creative Commons licence, unless indicated otherwise in a credit line to the material. If material is not included in the article's Creative Commons licence and your intended use is not permitted by statutory regulation or exceeds the permitted use, you will need to obtain permission directly from the copyright holder. To view a copy of this licence, visit <http://creativecommons.org/licenses/by-nc-nd/4.0/>.

circadian rhythms. At 640 days, altered DEGs in WD-fed female mice were associated with cardiac energy metabolism and remodeling.

Conclusions Our study demonstrated distinct sex-specific and age-associated differences in cardiac structure, function, and transcriptome signature between WD-fed male and female mice.

Keywords Western Diet, Sex, Heart, Cardiovascular, RNA sequencing

Graphical Abstract



Background

Cardiovascular diseases (CVDs) are one of the leading causes of morbidity and mortality worldwide [1, 2]. CVD develop because of the intricate interplay among genetic, environmental, and lifestyle factors [3, 4]. The local food environment, including factors such as dietary habits, the length of the food supply chain, and food contamination, significantly impacts health outcomes and cardiovascular risk. There is growing evidence suggesting that Western Diet (WD), defined by a high-fat and refined sugar (e.g., fructose and sucrose) content, is a significant risk factor for the development of CVDs, metabolic syndrome, neurodegenerative disorders, cognitive performance, and cancer [5–10].

To date, numerous epidemiological and animal studies have been conducted to elucidate the possible consequences of WD on pathophysiological and functional changes in the heart tissues, as well as the possible molecular mechanisms underlying these alterations [11–13]. Previous studies have demonstrated that, among other processes, WD affects inflammation, lipid metabolism, antioxidant status, and mitochondrial fitness through changes in gene expression and epigenetics that can

influence cardiovascular health [6, 13, 14]. Eight-week-old C57BL/6 male WD-fed mice have been shown to develop alterations in cardiac triglyceride dynamics and glucose tolerance, which initially presents with diastolic dysfunction that later in life shifts to the development of combined systolic (defined by reduced left ventricular ejection fraction; LVEF) and diastolic dysfunction [11]. This was paired with progressive metabolic remodeling, including the up-regulation of the key enzyme for ketone oxidation (BDH1), and alterations in the cardiac utilization of glucose due to reduced Glucose Transporter Type 4 (*GLUT4*) expression [11]. Long-term WD feeding also causes metabolic syndrome and in mice, that can contribute to the development of cardiac dysfunction and remodeling via dysregulation of caveolae and caveolin 1 (*CAV-1*) expression, lipotoxicity, and mitochondria-associated endoplasmic reticulum membrane disruption-associated cardiomyocyte apoptosis and endothelial dysfunction [12]. Furthermore, a study looking into the interplay of the gut-cardiovascular axis showed that WD-induced distinct changes in the expression of genes related to lipid metabolism (*SCD*, *FADS1*, and *SQLE*), interferon signaling, and inflammation in the jejunum of

Ossabaw pigs was associated with the severity of atherosclerotic lesions and serum cholesterol levels, though the authors noted these observations might have been due to collinearity [15]. The 'inflammatory power' of diet is well-documented in several studies, and the calculation of the dietary inflammatory index is recommended to integrate diet and inflammation for assessing cardiovascular risk [16, 17].

The studies on sex-specific responses to WD in wild-type mice (i.e., C57Bl6/J strain) are relatively scarce. However, it has been reported that male and female mice exhibit differences in their blood and urine metabolomes, resistance in arteries under acute oxidative stress, caspase-1 activation patterns, inflammatory phenotypes, lipid profiles, and susceptibility to non-alcoholic fatty liver disease when fed WD [18–20]. It was demonstrated that male metabolic syndrome rats exhibited significantly greater impairment in cardiac function compared to females. However, the WD diet abolished the female-specific protective effect, with the observed cardiac impairment being linked to oxidative stress [21]. Lower cardiac mitochondria numbers in female rats are associated with reduced free radical production and decreased oxidative damage [22]. Cardiovascular sexual dimorphism has been observed in both human and rodent studies under diet-induced conditions. In Nile rats, males demonstrate a higher susceptibility to diastolic dysfunction when fed a Western-style diet, even without systemic evidence of type 2 diabetes or metabolic syndrome, while females show resilience to these changes [23]. Similarly, human population studies reveal that although men and women have comparable lifetime risks of cardiovascular disease, men are more likely to develop coronary heart disease earlier, whereas women are more prone to cerebrovascular disease or heart failure later in life [24]. These findings highlight the importance of sex-specific responses to diet and metabolic stressors in understanding cardiovascular disease risk and progression which underscore the importance of tailoring lifestyle interventions to account for sex-specific differences. Men may benefit more from strategies focused on metabolic control and weight management, whereas women may achieve greater risk reduction through lifestyle changes targeting increased physical activity, blood pressure regulation, and cholesterol management. Recognizing these differences is crucial for optimizing lifestyle-based approaches to reduce cardiovascular risk. Age-related increases in arterial stiffness, blood pressure, and prevalence of CVD are generally considered unavoidable consequences of aging [25]. Furthermore, research has shown that aortic lesions caused by aging could be aggravated by WD [26].

Although several investigations have explored the cardiovascular complications triggered by the consumption of a WD, additional research is essential to understand

the long-term effects of WD on cardiac structure and function and the underlying molecular pathways contributing to these alterations. In this study, we aimed to investigate the long-term (i.e., murine lifetime) sex-specific gene expression patterns in LV tissue using a transcriptomic approach in male versus female WD-fed C57BL/6 J mice (continuously for 125 days) at a relatively young age, from 300 through 425 days old.

Methods

Mice groups

We used C57BL6/J mice to evaluate the long-term effects of WD on CVD development in wild-type (WT) mice (notwithstanding that WT mice are more resistant than genetically modified murine atherosclerosis models, Apolipoprotein E (ApoE) or low-density lipoprotein receptor (LDLR) knockout mice for development of atherosclerosis). For RNA sequencing studies, the WD-fed group (n=20, male/female:10/10, randomly selected) was fed a custom Teklad diet containing 42% fat (TD.88137, <https://insights.envigo.com/hubfs/resources/data-sheets/88137.pdf>) (Envigo, Madison, WI) for 125 days from ages 300 to 425 days (mice were 90 days old when purchased from Jackson Labs and arrived to our vivarium). Our selection was based on a life phase equivalence of 300–420 days for mice, corresponding to 38–47 years for humans [27]. Likewise, for RNA sequencing, the Normal diet (ND)-fed (n=20, male/female:10/10, randomly selected) mice served as negative controls and were fed a standard chow diet ad libitum (Fig. 1). Please note that experiment was started with a larger number of mice for both sexes and diets, but 10 mice per sex/treatment group were used for longitudinal echocardiography studies, and a different set of 5 mice per sex/treatment group was used for RNA sequencing studies at each timepoint. The absolute number of mice at the start of experiments as well as the number of mice at the collection times, are presented in Supplemental Table S1.

Echocardiography

Transthoracic echocardiography to assess cardiac structure and function was performed using a GE Vivid E9 with XDclear Cardiac Ultrasound (General Electric Company, Boston, MA, USA) with a GE model i13L pediatric cardiac probe (General Electric Company). ECHO was conducted on all groups at 455, 530, and 750/640 days (male/female, 10/10 for each sex and time point). Mice were anesthetized with isoflurane (Baxter Healthcare Corporation, Deerfield, IL, USA)—induced at 3% and maintained with 1–2%. Hair was removed from the neckline to the mid-chest (using Nair). Mice were then placed supine on a heated table to maintain a core temperature of 37 °C. B- and M-mode images were acquired from a parasternal short-axis view to evaluate the left ventricular

Study design

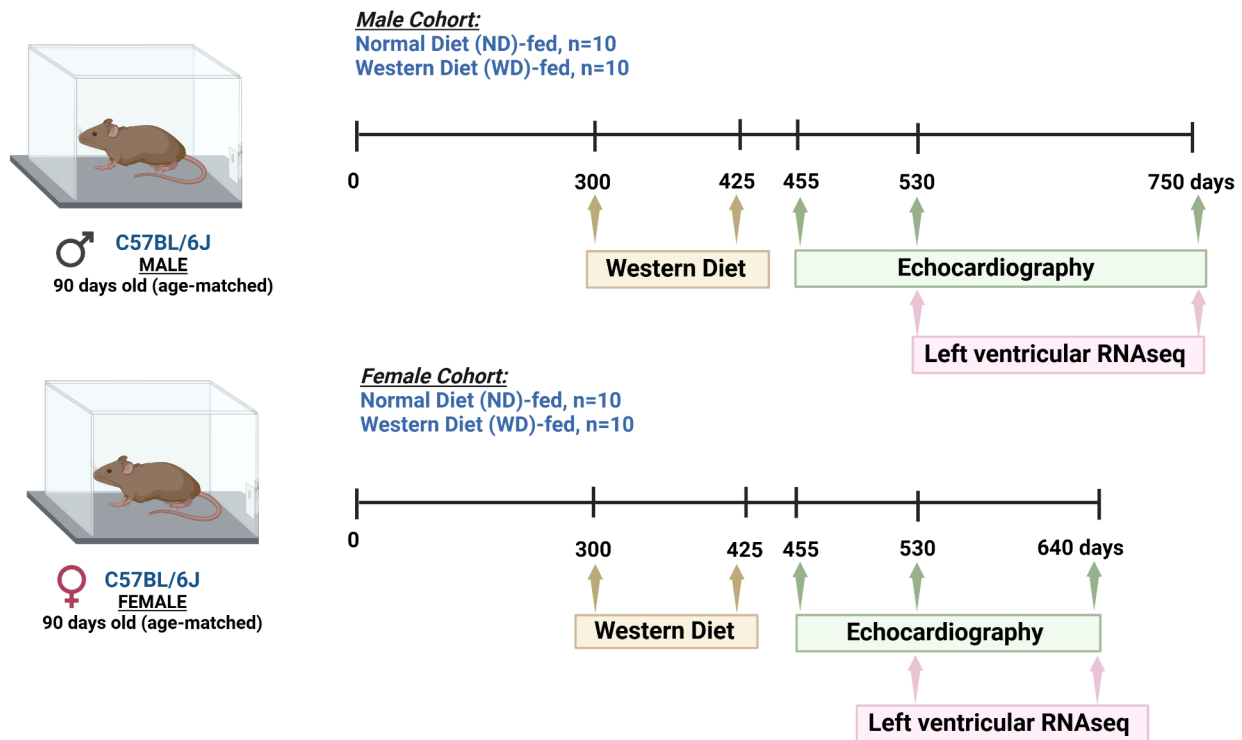


Fig. 1 Study design overview: timeline and methodology. Wild Type C57BL/6J male and female mice were fed normal (ND) or a western diet (WD) for 150 days (n = 10 mice in each group). Transthoracic echocardiography was performed on all mice at 455, 530, and 750/640 days. Bulk mRNA sequencing was performed on left ventricular cardiac tissue samples collected at 530 and 750 days for male mice (n = 5 mice in each group), and 530 and 640 days for female mice (n = 5 mice in each group)

(LV) ejection fraction (EF), LV fractional shortening (FS), end-systolic (ESV), and end-diastolic volumes (EDV), LV end-diastolic diameter (LVEDd), LV end-systolic diameter (LVESD), posterior wall thickness at end-diastole (LVPWd) and systole (LVPWs), intraventricular septal thickness (IVSd), LV internal diameter at end diastole (LVIDd), and LVID at end systole (LVIDs), LV mass ($1.053 \times ((LVIDd + PWthd + IVSd)^3 - LVIDd^3)$), radial wall strain (DWS; $[IVSd + LVPWd] / LVIDd$), and relative wall thickness (RWT; $((2 \times LVPWd) / LVIDd)$). Of note, each ECHO parameter is reported as an average of three individual measurements (not repeated measures).

qRT-PCR

Total RNA was extracted from the LV tissues of both male and female mice at 530, 750- and 640-days of age fed either a normal diet (ND) or a Western diet (WD) using TRIzol reagent (Invitrogen, #15596018, Thermo Fisher Scientific, Waltham, MA, USA). The cDNA was then synthesized using qScript cDNA SuperMix (Quantabio, #95048) according to the manufacturer's protocol. Quantitative PCR (qPCR) was conducted using PowerTrack™ SYBR Green Master Mix (Applied Biosystems,

#A46109) as per the manufacturer's instructions. mRNA expression levels were normalized against GAPDH. Primer sequences are detailed in the Supplemental Table S2.

RNA extraction, library preparation, and sequencing

Total RNA was extracted from LV tissues using the RNeasy Mini Kit (Qiagen, USA) according to the manufacturer's instructions and stored at -80°C until further use. A Poly-A selected mRNA library was prepared with NEBNextUltra™II RNA Library Prep Kit. RNA sample quality check (RNA integrity number (RIN), concentration) and validation of the libraries were performed using an Agilent Bioanalyzer and qPCR. The Bioanalyzer was used to assess the size and quality of the library, while qPCR was used to quantify the library concentration and verify the presence of Illumina anchor sequences. The sequencing was performed on the Illumina NovaSeq-6000 platform with an average of 23–52 million 2×150 bp paired-end raw reads per sample, with $>93\%$ of QC30 and $>46\%$ GC count (Supplemental Table S3).

Data processing

FastQC (version 0.11.9) was used for the quality assessment of raw sequencing reads (<https://www.bioinformatics.babraham.ac.uk/projects/fastqc/>). Next, we aligned the reads to the mouse reference genome (mm39) with STAR aligner (version 2.7.8a) [28] with gene count quantification mode and obtained raw gene counts. On average 90.48% of the reads were mapped to the reference genome. The adapter sequence was not trimmed. Raw gene count data was filtered to exclude genes with lower than 10 counts present in more than 10 samples.

Statistics

Echocardiography parameters were analyzed using an unpaired t-test with data-passing assumptions required for normality (Shapiro–Wilk) and heteroscedasticity (Brown–Forsythe). All analyses were performed using GraphPad Prism 8, version 8.4.3 (GraphPad Software, Inc, La Jolla, CA, USA). Data are expressed as mean \pm SEM, except in box plots where whiskers extend from minimum to maximum. Differences were considered statistically significant at $p < 0.05$. Differential gene expression analysis was performed from raw gene counts using the DESeq2 R package (version 1.42.1) (<https://bioconductor.org/packages/release/bioc/html/DESeq2.html>) [29]. After normalization, scaling, and estimation of global variance, the differential gene expression was analyzed as follows: 530 days ND vs WD males; 750 days ND vs WD males; 530 days ND vs WD females; 640 days ND vs WD females. Genes with $FDR < 0.05$ were considered as differentially expressed. The overrepresentation analysis of KEGG pathways was performed using the entichr R package [30].

Results

Pathological assessment of longitudinal mortality in treatment groups

Compared to male mice, female mice exhibited higher mortality between 360 and 530 days of age, with a large proportion of mice found spontaneously dead. Autopsies of animals found dead or euthanized between 360 and 530 days timepoints showed a larger distribution of pathological diagnoses with a somewhat higher incidence of cancer (metastatic lymphoma, hemangiosarcoma, and hepatocellular carcinoma) in male and female WD-fed mice than normal diet (ND)-fed controls (Supplemental Table S4). However, no specific unifying diagnosis for cause of death was identified to explain higher rates of mortality in the female cohort. Therefore, the final timepoint collection for female ECHO data and heart LV samples was limited to 640 days to ensure that we had a significant number of animals in each group for adequate interpretation of the results.

Effect of western diet on LV structure and function

To assess the long-term degenerative effects of WD on LV function, we performed echocardiography at 455, 530, and 640/750 days of age in both male and female murine cohorts. Throughout image acquisition, compared to ND-fed male mice, there was no significant difference in heart rate or other physical parameters such as total body weight or heart weight in WD-fed mice (Fig. 2A–C). At both 455 and 530 days of age, there was no significant difference in LV function in male WD-fed mice compared to controls (Fig. 2E–H). However, LV interventricular septal thickness (IVSD) was significantly increased at 530 days in WD-fed mice, suggesting possible cardiac remodeling at this time ($p < 0.02$) (Fig. 2J). In male mice, the effects of WD were observed only at 750 days of age, where WD-fed mice exhibited significantly reduced global LV systolic function (LVEF: $42\% \pm 14$ WD vs. ND $60\% \pm 7$, $p = 0.0005$; LVFS: $18\% \pm 7$ WD vs. ND $27\% \pm 5$, $p = 0.0106$) (Fig. 2E and F) with no detectable structural alterations (Fig. 2H–M).

Across all groups in the female cohort, no significant differences were observed in physiologic parameters, including heart rate, body weight, or heart weight, which could contribute to variation in echocardiography interpretation (Fig. 2O–R). Across all stages of life (i.e., at 455, 530 or 640 days of age), there was no significant difference in global systolic function, defined by LVEF or LVFS, between female mice fed a ND or WD (Fig. 2S and T). While no structural changes were observed between both female cohorts at 455 days of age, alterations in LV size, including LV total and internal cavity diameter, as well as LV mass were significantly increased in WD-fed female mice at 530 days of age compared to controls (LVEDd: 6.2 ± 0.8 mm vs. ND 5.4 ± 0.6 mm, $p = 0.0237$; LVIDd: 4.1 ± 0.6 mm vs. ND 3.4 ± 0.3 mm, $p = 0.0098$; LV mass: 184 ± 75 mg vs. ND 124 ± 38 mg, $p = 0.0365$) (Fig. 2W, Z, AB). This was paired with a significant 1.5-fold increase in SV, which may have been a compensatory increase considering enlargement in LV cavity size and preservation in LVEF ($p = 0.0139$) (Fig. 2S, T, U, Z); however, further direct hemodynamic assessment is warranted to verify alterations in preload and afterload. This change in LV size; however, was not paired with changes in septal or posterior wall thickening, likely reflecting dilatory rather than hypertrophic remodeling ($p < 0.05$) (Fig. 2W, X, Y). By 640 days of age, there is a significant decrease in DWS along with decreased RWT in WD-fed mice, suggesting possible development of myocardial stiffness and dilated LV remodeling ($p = 0.0125$) (Fig. 2V, AA), though further assessment of diastolic function would be required using Doppler to further assess this.

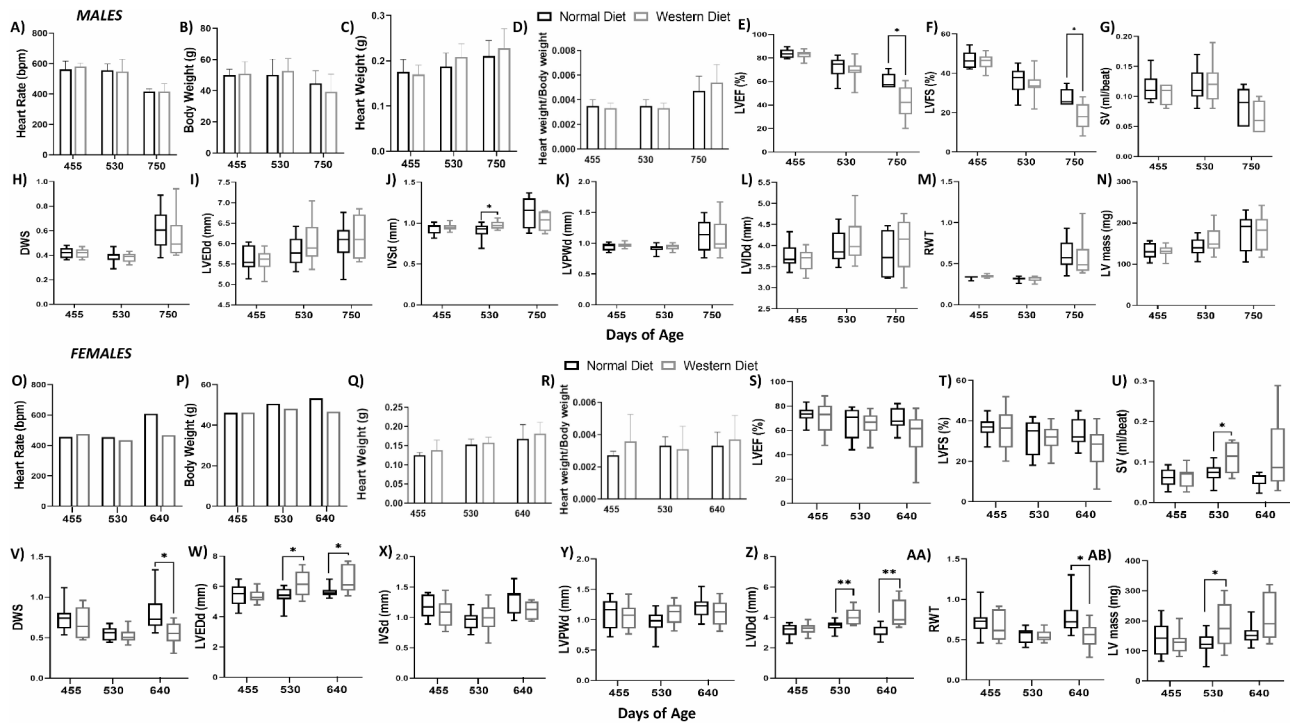


Fig. 2 Longitudinal echocardiography results in C57BL/6 J male and female mice fed with ND and WD. We assessed left ventricle (LV) function by transthoracic echocardiography (ECHO) at 455, 530, and 640/750 days. Normal diet (ND)-fed mice served as negative control. *LV function and structure in male mice:* (A) Heart rates were obtained during ECHO while mice were anesthetized using isoflurane (3% induction, 1–2% maintenance), (B) Mice body weights. (C) Heart weight (D) Heart weights/Body weight ratio. Left Ventricular (LV) function is represented by (E) ejection fraction, (F) fractional shortening, (G) stroke volume (SV), and (H) radial wall strain (DWS). Parameters of LV dimensions and remodeling are represented by (I) LV end diastolic diameter, (J) intraventricular septal thickness, (K) LV posterior wall thickness, (L) LV internal cavity diameter, (M) relative wall thickness, and (N) LV mass. N=7–10 animals; p-values were calculated using unpaired t test. * $p < 0.05$. *LV function and structure in female mice:* (O) Heart rates, (P) Mice body weights. (Q) Heart weight (R) Heart weights/Body weight ratio. Left Ventricular (LV) function is represented by (S) ejection fraction, (T) fractional shortening, (U) stroke volume (SV), and (V) radial wall strain (DWS). Parameters of LV dimensions and remodeling are represented by (W) LV end diastolic diameter, (X) intraventricular septal thickness, (Y) LV posterior wall thickness, (Z) LV internal cavity diameter, (AA) relative wall thickness, and (AB) LV mass. N=7–10 animals; p-values were calculated using unpaired t test. * $p < 0.05$

Cardiac remodeling, calcium signaling, inflammation and hemodynamic stress gene expression in female and male heart tissue

Quantitative PCR analysis of LV tissues from male and female mice at 640 or 750 days fed either a normal or western diet revealed distinct gene expression patterns. In males, markers for cardiac fibrosis, calcium handling, and inflammation did not significantly change despite a modest upward trend following a western diet (Fig. 3A, B, C). Similarly, markers of cardiac remodeling, such as *Mmp9*, *Galectin 3*, and β -*Mhc*, along with hemodynamic stress markers *Anp* and *Bnp*, were slightly up-regulated, but not to a statistically significant extent (Fig. 3D, E). In contrast, female mice displayed a significant response to the Western Diet. The expression of *Tgfb* and *Col3a1*, critical fibrotic markers, was significantly elevated in females, indicating increased cardiac fibrosis signaling compared to that in males (Fig. 3F). There was also a notable increase in calcium-handling genes *Ncx* and *Serca2a* and the inflammatory marker *Mcp1* (Fig. 3G, H). Genes associated with cardiac remodeling, including

Mmp9 and β -*Mhc*, were also elevated, suggesting active cardiac structural changes (Fig. 3I). Importantly, the hemodynamic stress markers *Anp* and *Bnp* were significantly higher in females (Fig. 3J), consistent with the pronounced structural changes observed by echocardiography in female mice (Fig. 2V, W, Z, AA, AB). Overall, the differential gene expression between males and females suggests sex-specific cardiac responses to dietary challenges. Indeed, the significant upregulation of genes related to fibrosis, calcium handling, inflammation, and remodeling in females underscores their increased susceptibility to diet-induced cardiac stress. This sex disparity aligns with our echocardiographic findings, which indicated more pronounced structural changes in the left ventricles of females. Taken together, our data emphasize the importance of considering sex as a critical variable in studies of diet-induced cardiac pathologies.

Principal component analysis of mRNA sequencing data

Principal component analysis (PCA) identified the first 15 principal components (PCs) to explain 50% of the

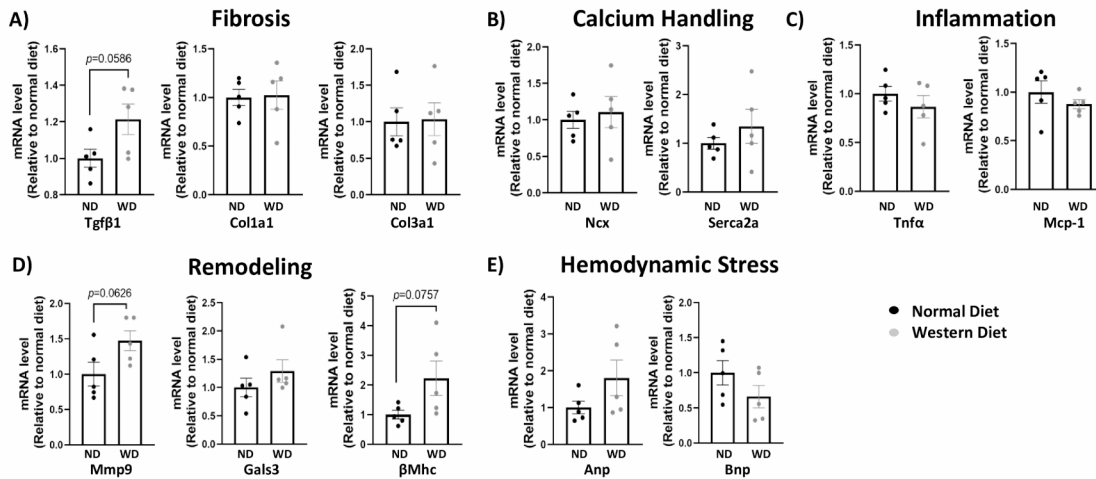
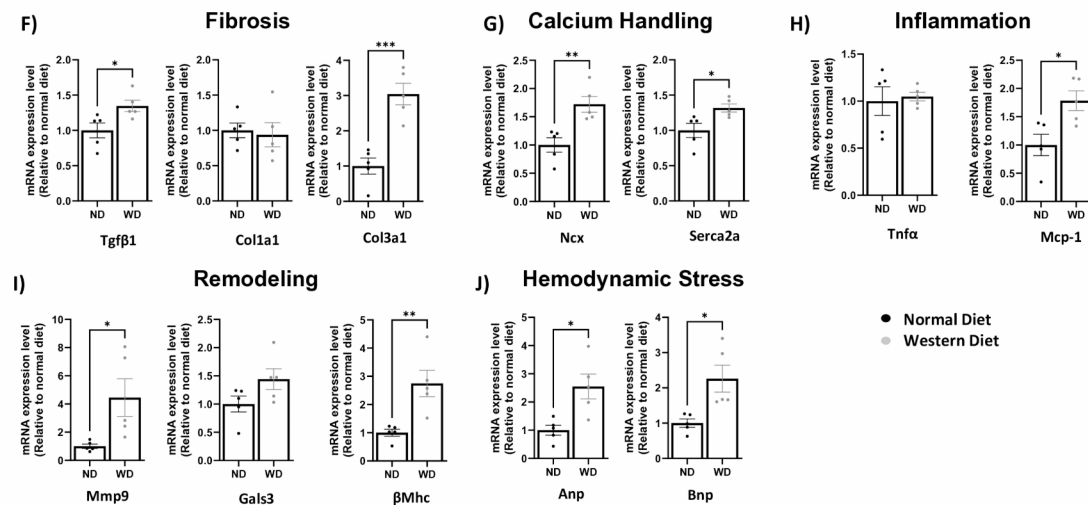
MALES**FEMALES**

Fig. 3 Gene expression analyses in LV tissue from male and female mice at 750/640 day fed with normal versus western diet. Gene expression was assessed for: **A** Cardiac fibrosis markers: Tgfb1 (transforming growth factor beta 1), Col1a1 (type I fibrillar collagen), and Col3a1 (type III fibrillar collagen). **B** Calcium handling proteins: Ncx (cardiac sodium-calcium exchanger) and Serca2a (Sarcoplasmic Reticulum Ca²⁺ ATPase). **C** Inflammation markers: TNFα (tumor necrosis factor alpha) and MCP1 (monocyte chemoattractant protein-1). **D** Cardiac remodeling enzymes: Mmp9 (matrix metalloproteinase-9), Gals3 (galectin 3), and βMhc (cardiac beta myosin heavy chain). **E** Hemodynamic stress hormones: Anp (atrial natriuretic peptide) and Bnp (brain natriuretic peptide). Expression levels were normalized to GAPDH. Data are presented as mean ± SEM. Each dot represents an individual mouse, with n = 5 animals per diet group. Statistical significance was assessed using an unpaired t-test, **p* < 0.05, ***p* < 0.01, ****p* < 0.001

variance in the expression data. Notably, the second PC was associated with sample collection time and RIN, while PC5 was associated with sex and PC39 with diet (Fig. 4A). Further, high-dimensional clustering and visualization on uniform manifold approximation and projection (UMAP) revealed distinct expression patterns based on sex, diet, and sample collection time (Fig. 4B-D, respectively). Based on this, we conducted differential expression analysis with adjustment for RIN and stratification by sex and sample collection time. Thus, mRNA expression levels in the LV tissue of WD groups collected at 530 and 750 days for males and females at 530

and 640 days were compared with those of the ND age-matched male and female mice groups.

Genes with distinct expression patterns in the LV of the heart among the study groups

Differential expression analysis across the four comparisons in our study revealed the highest number of DEGs (1,408) in the 530 days WD-fed male group compared to the 530 days male ND-fed mice (Fig. 5A, Table 1, Supplemental file 2: spreadsheet 1). In total, 753 up-regulated and 618 downregulated transcripts were identified comprising protein-coding (594 up- and 692 downregulated)

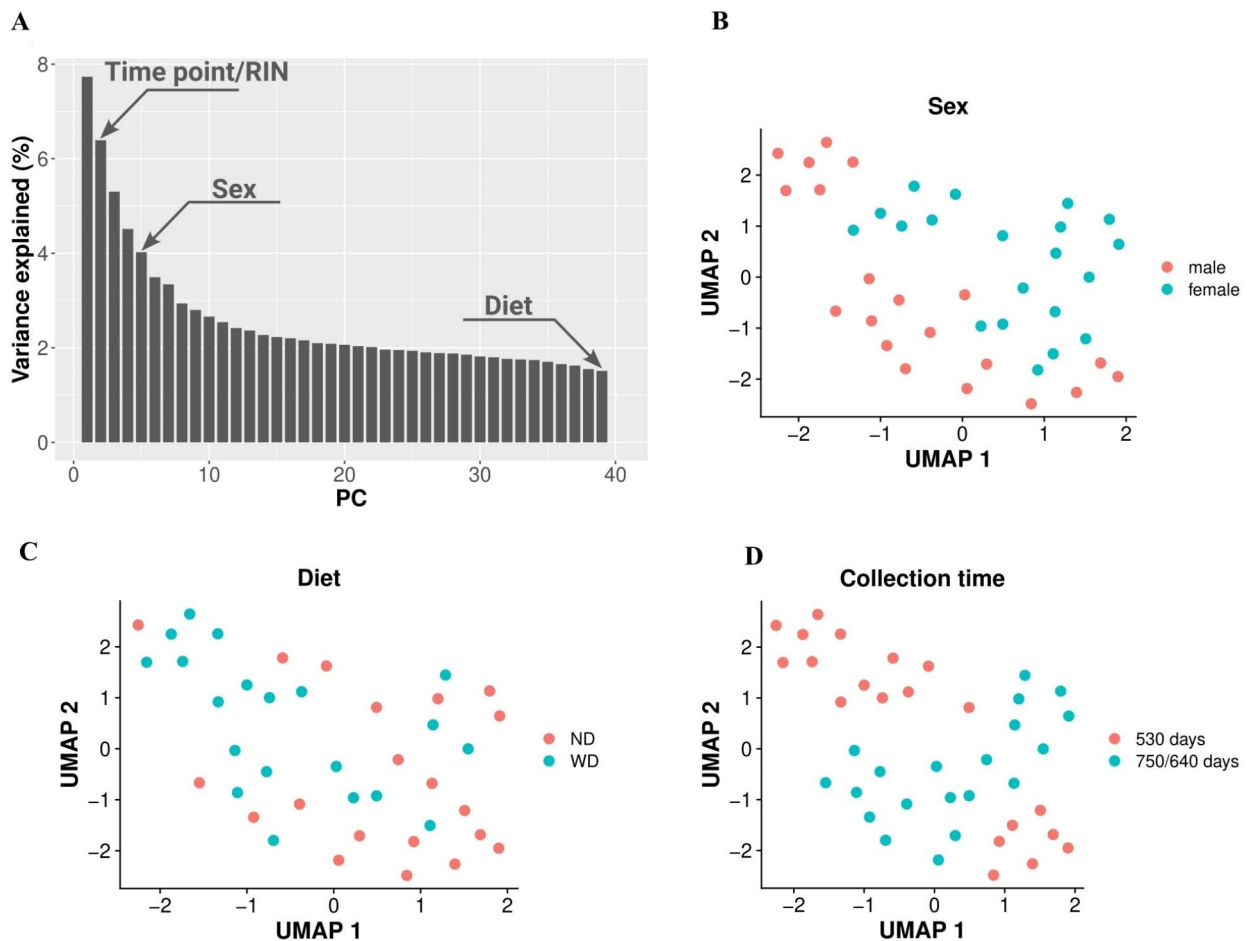


Fig. 4 Analysis of principal components and UMAP clustering of left ventricular mRNA expression data. **A** Elbow plot illustrating the variance percentages explained by each principal component. Annotated bars indicate the principal components that exhibit the most significant separation for the specified condition. **B–D** Uniform manifold approximation and projection (UMAP) clustering of left ventricular mRNA expression data. Each dot represents a sample, with color coding corresponding to sex (**B**) (male/female; red/green), age (**C**) (530 and 750/640 days; red/green), and dietary regimen (**D**) (normal diet (ND)/western diet (WD)); red/green)

and long non-coding RNA (lncRNAs) (24 up- and 61 downregulated) genes (Table 1, Supplemental file 2: spreadsheet 1). The DEGs identified in the 530 days WD-fed male group have been previously associated with various cardiac structural abnormalities (*Myh6*, *Myh7*, *Prkg1*, *Dhcr7*, *Ttn*, *Actg1*, *Dmd*, *Itga1*, *Itga3*, *Itga4*, *Itga7*, *Itgav*, *Pkp2*), abnormal LV morphology (*Eftud2*, *Il17rd*), and enlarged heart (*Amigo3*). Additionally, we observed significant upregulation of genes associated with decreased heart rate (*Il33*, *Zbtb37*, *Zbed6*, *Adra1a*) and downregulation of transcripts involved in increased heart rate (*Fhod1*, *Hnrnpm*). We found underexpression of genes associated with disrupted calcium homeostasis (*Cacna1h*, *Cacnb2*, *Slc39a2*, *Fam222a*), potentially impacting cardiac function. Additionally, five genes related to DNA repair (*Ercc2*, *Hnrnpa3*, *Vcpip1*, *Rif1*, *Ercc1*) and two lncRNAs (*Airn*, *Kcnq1ot1*) associated with abnormal DNA methylation showed differential expression in

the 530 days WD-fed male group, suggesting possible epigenetic and DNA repair dysregulation in heart tissue. Moreover, among the transcripts in this group exhibiting altered expression levels, 85 were annotated as lncRNA genes (24 up- and 61 downregulated) (Supplemental file 2: spreadsheet 1). The analysis of target genes revealed in total 74 DEGs regulated by 23 lncRNAs (10 up- and 13 downregulated) (Supplemental file 3: spreadsheet 1). All these lncRNAs were reported to target the *Upf1* gene, which is involved in mRNA cytoplasmic degradation and maintenance of genome stability [31]. Furthermore, we found significant upregulation of *Malat1* lncRNA, which, according to our analysis, is interacting with the 24 protein-coding DEGs (Supplemental file 3: spreadsheet 1). Interestingly, these transcripts are reported to be dysregulated in various types of cancers, and in regulation of RNA expression and epigenetics [32, 33]. However, further studies focusing on the non-coding transcriptome

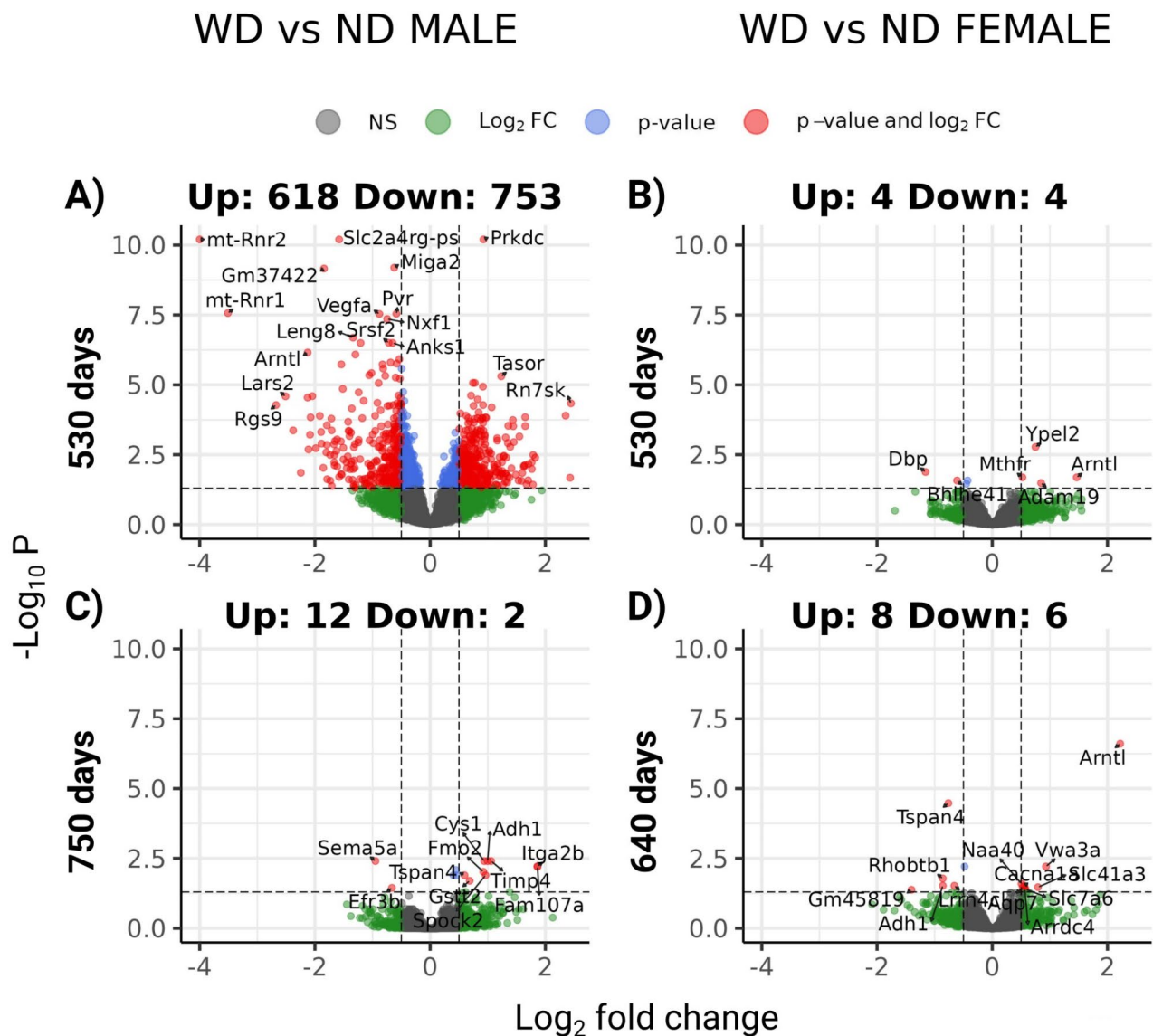


Fig. 5 Differentially expressed genes (DEGs) across study groups are represented as volcano plots. **A** 530 days normal diet (ND) vs western diet (WD) males, **B** 750 days ND vs WD males, **C** 530 days ND vs WD females, **D** 640 days ND vs WD females. Volcano plot of data with log base 2-transformed fold change values plotted on the X-axis and negative log₁₀ p values plotted on the Y-axis, representing the significance level. The dotted horizontal line signifies $p=0.05$ ($-\log_{10}(1.3)$). The two vertical lines correspond to a fold change of 2 (-2), with up-regulated and downregulated genes plotted on the right and left sides of these lines, respectively

are needed to elucidate the epigenetic mechanisms underlying these observed changes.

As for the other three comparisons, the number of DEGs identified in these analyses was significantly lower and did not reveal lncRNA (Fig. 5B–D, Table 1). The DEGs observed in 750 days male ND-fed group compared to the 750 days male WD-fed group (12 up- and 2 down-regulated) are mainly involved in abnormal heart (*Timp4*) and blood vessel morphology (*Sema5a*), ethanol metabolism (*Adh1*), and coagulation (*Itga2b*) (Fig. 5B, Table 1, Supplemental file 2: spreadsheet 2). Only eight DEGs (4 down- and 4 up-regulated) were observed in LV tissue of 530 days WD-fed female mice compared to those in

the ND-fed female group (Fig. 5C, Table 1, Supplemental file 2: spreadsheet 3). Interestingly, three of the genes are associated with the circadian clock and immune cell differentiation (*Arntl*—up-regulated, *Bhlhe41* and *Dbp*—down-regulated), and one up-regulated gene (*Mthfr*) is related to abnormal blood homeostasis. As for the 640-day WD-fed female group, there were 13 protein-coding DEGs (8 up- and 5 down-regulated) in this group when compared with 640 days ND-fed female mice. These genes are reported to be associated with the alterations in B cell differentiation (*Arntl*), kidney, thyroid gland, and lymph nodes morphology (*Aqp7*, *Rhobtb1*, and *Arrdc4*, respectively), formation of blood vessels (*Angptl2*) as

Table 1 The top up- and downregulated differentially expressed genes in all comparison groups

Gene type	Gene symbol	Gene description	Log2FC	padj	
<i>530 days male mice ND vs. WD</i>					
Protein coding	<i>Zbed6</i>	zinc finger, BED type containing 6	2.43	2.1E-02	
	<i>Sfn3</i>	schlafen 3	2.35	1.3E-04	
	<i>Zbtb37</i>	zinc finger and BTB domain containing 37	1.83	4.0E-03	
	<i>Hipk2</i>	homeodomain interacting protein kinase 2	1.78	3.7E-02	
	<i>Lcor</i>	ligand dependent nuclear receptor corepressor	1.77	1.0E-02	
	<i>Rgs9</i>	regulator of G-protein signaling 9	-2.68	5.3E-05	
	<i>Lars2</i>	leucyl-tRNA synthetase, mitochondrial	-2.51	2.6E-05	
	<i>Hbb-bt</i>	hemoglobin, beta adult t chain	-2.24	1.4E-02	
	<i>Arntl</i>	aryl hydrocarbon receptor nuclear translocator-like	-2.13	7.0E-07	
	<i>Spon2</i>	spondin 2, extracellular matrix protein	-2.11	2.1E-03	
	lncRNA	<i>Gm15564</i>	predicted gene	1.79	3.2E-03
		<i>4632427E13Rik</i>	RIKEN cDNA 4632427E13 gene	1.63	8.6E-03
		<i>Kcnq1ot1</i>	KCNQ1 overlapping transcript 1	1.55	7.0E-04
		<i>Lncpint</i>	Trp53 induced transcript	1.45	1.1E-03
<i>5930430L01Rik</i>		RIKEN cDNA 5930430L01 gene	1.44	3.0E-04	
<i>Gm27028</i>		predicted gene	-2.38	4.3E-04	
<i>Gm14286</i>		predicted gene	-2.13	2.9E-05	
<i>Mir17hg</i>		Mir17 host gene (non-protein coding)	-2.07	1.5E-04	
<i>Gm56503</i>		predicted gene	-1.91	1.3E-04	
<i>Gm31619</i>		predicted gene	-1.89	4.9E-04	
<i>750 days male mice ND vs. WD</i>					
Protein coding	<i>Fam107a</i>	family with sequence similarity 107, member A	1.86	6.3E-03	
	<i>Itga2b</i>	integrin alpha 2b	1.86	6.1E-03	
	<i>Timp4</i>	tissue inhibitor of metalloproteinase 4	1.06	3.9E-03	
	<i>Adh1</i>	alcohol dehydrogenase 1 (class I)	1.00	3.9E-03	
	<i>Spock2</i>	sparc/osteonectin, cwcv and kazal-like domains proteoglycan 2	0.96	1.3E-02	
	<i>Sema5a</i>	sema domain, seven thrombospondin repeats trans-membrane domain (TM) and short cytoplasmic domain, (semaphorin) 5A	-0.95	3.9E-03	
	<i>Efr3b</i>	EFR3 homolog B	-0.66	3.6E-02	
<i>530 days female mice ND vs. WD</i>					
Protein coding (meltrin beta)	<i>Arntl</i>	D site albumin promoter binding protein	1.47	2.0E-02	
	<i>Adam19</i>	aryl hydrocarbon receptor nuclear translocator-like	0.85	3.3E-02	
	<i>Ypel2</i>	a disintegrin and metalloproteinase domain 19			
	<i>0.75</i>	1.7E-03			
	<i>Mthfr</i>	yippee like 2	0.52	2.0E-02	
	<i>Dbp</i>	D site albumin promoter binding protein	-1.16	1.3E-02	
	<i>Bhlhe41</i>	basic helix-loop-helix family, member e41	-0.61	2.7E-02	
	<i>Slc45a4</i>	solute carrier family 45, member 4	-0.45	3.5E-02	
	<i>Ifrd2</i>	interferon-related developmental regulator 2	-0.43	2.7E-02	
<i>640 days female mice ND vs. WD</i>					
Protein coding	<i>Arntl</i>	aryl hydrocarbon receptor nuclear translocator-like	2.22	2.5E-07	
	<i>Vwa3a</i>	von Willebrand factor A domain containing 3A	0.93	6.2E-03	
	<i>Slc41a3</i>	solute carrier family 41, member 3	0.79	3.4E-02	
	<i>Slc7a6</i>	solute carrier family 7 (cationic amino acid transporter, y+ system), member 6	0.58	4.0E-02	
	<i>Arrdc4</i>	arrestin domain containing 4	0.56	4.0E-02	
	<i>Rhobtb1</i>	Rho-related BTB domain containing 1	-0.86	1.7E-02	
	<i>Adh1</i>	alcohol dehydrogenase 1 (class I)	-0.86	3.0E-02	
	<i>Tspan4</i>	tetraspanin 4	-0.76	3.3E-05	
	<i>Lrrn4cl</i>	LRRN4 C-terminal like	-0.66	3.0E-02	
	<i>Angptl2</i>	angiopoietin-like 2	-0.48	6.2E-03	

well as ethanol metabolism (*Adh1*). Circadian clock gene *Arntl*, also known as *BMAL1*, was up-regulated at both 530 and 640 days in WD-fed female mice (Fig. 5D, Table 1, Supplemental file 2: spreadsheet 4).

Several DEGs were found to overlap across four comparisons (Fig. 6A). The UpSet plot shows an overlap in four different comparisons (Fig. 6B). In male mice, three genes (*Cys1*, *Fmo2*, *Pik3ip1*) showed significant upregulation in response to the WD, while the expression of two other genes (*Tspan4*, *Adh1*) was significantly different in all WD mice except for 530 days WD females (Fig. 6B). Finally, three protein-coding DEGs (*Vwa3a*, *Slc41a3*, *Aqp7*) were identified as common between 530 days male and 640 days female WD-fed mice, and *Arntl* was common in all comparison groups except for the 750 days WD-fed males (Fig. 6B). Interestingly, seven intersecting DEGs (*Tspan4*, *Adh1*, *Vwa3a*, *Slc41a3*, *Aqp7*, *Arntl*, *Gm45819*) showed opposite expression patterns between

males and females. Taken together, these DEG patterns suggest potential differences in the molecular response to the WD between sexes.

Pathways dysregulated in the LV of 530 days WD male group

We performed pathway overrepresentation analysis of DEGs in all comparison groups. The only significant enrichment results were obtained in 530-day ND vs. WD-fed male groups. The overrepresentation analysis of protein-coding DEGs identified 12 dysregulated KEGG pathways (Fig. 7, Supplemental file 3: spreadsheet 2). Among them, we noted a considerable number of genes enriched in spliceosome KEGG pathway and signal transduction pathways such as cGMP-PKG, Notch, and phospholipase D. These pathways play crucial roles in endocrine system alterations (glucagon, insulin resistance, AGE-RAGE signaling pathway in

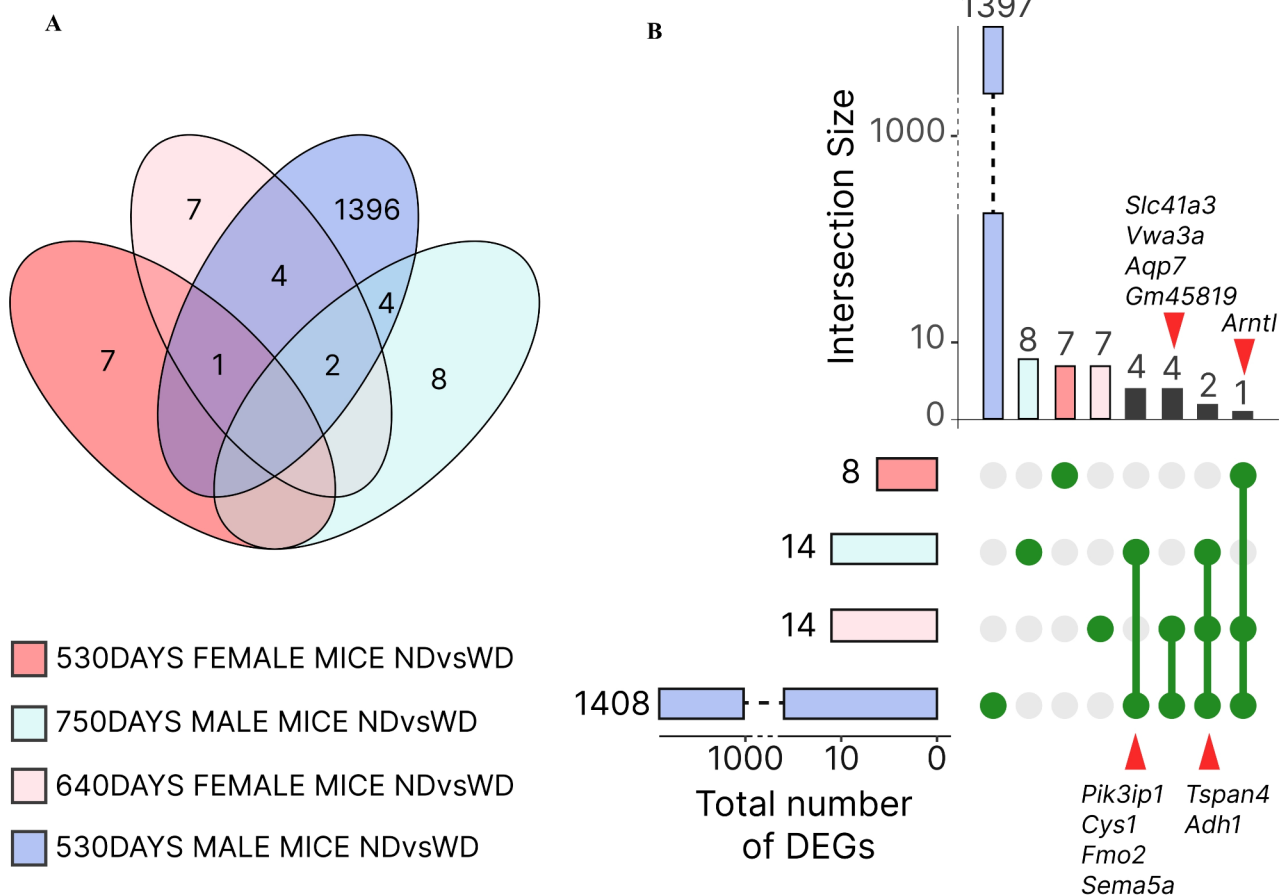


Fig. 6 Number of overlapping and unique differentially expressed genes (DEGs) between comparison groups. **A** The number of DEGs for each comparison, as well as overlapping DEGs between groups. **B** UpSet plot summarizes differentially expressed gene overlaps in four different comparisons (normal diet (ND) vs western diet (WD) for 530 days females; ND vs. WD for 750 days males; ND vs. WD 640 days females; ND vs. WD 530 days males). The horizontal bar graph at the bottom left, labeled 'Set Size', illustrates the total number of DEGs on the X-axis, categorized by each comparison on the Y-axis. The top vertical graph represents the intersection of gene sets. Each column corresponds to a specific comparison (first four columns), and instances where more than one comparison share the same DEGs are indicated by dots connected by lines below the X-axis

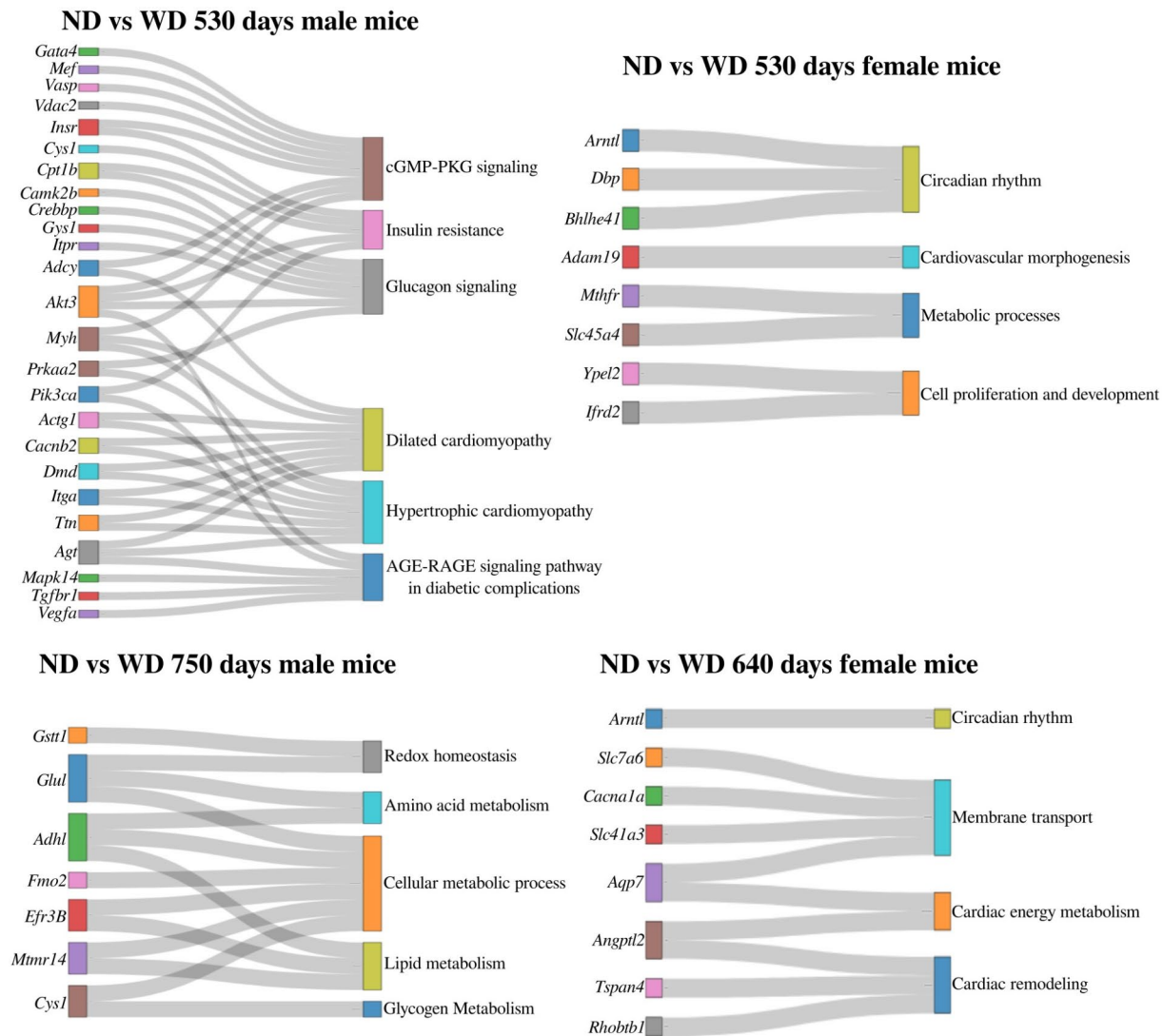


Fig. 7 Top differentially regulated genes in the four comparison groups, along with the pathways and processes in which they are enriched. Four Sankey plots represent the following comparisons: normal diet (ND) vs western diet (WD) 530 days male mice, ND vs. WD 750 days male mice, ND vs. WD 530 days female mice, and ND vs. WD 640 days female mice. The left side illustrates the genes, which are linked to the corresponding processes and pathways on the right side

diabetic complications). Additionally, there was significant enrichment of pathways related to CVDs, including dilated and hypertrophic cardiomyopathies (Fig. 7, Supplemental file 3: spreadsheet 2).

Discussion

The effect of high-fat and high-sugar diets on cardiac function has been documented in several animal studies [34, 35]. Most animal studies investigating the life-long effects of a WD have primarily involved male mice. However, differences in hormonal levels, fat distribution, and mitochondrial bioenergetics due to sex dimorphism can contribute to variations in the metabolic response

to the WD between sexes [20, 36, 37]. In this study, we examined the long-term effect of WD on the functional and structural alterations of the LV and its transcriptome in male and female C57BL/6 J mice. We found that WD consumption had a long-lasting effect on LV in male mice manifested by systolic dysfunction. In contrast, WD female mice showed more prominent structural changes, including dilatation, hypertrophy, and an increased DWS, suggesting possible development of diastolic dysfunction. Additionally, we found that sex-specific alterations in LV structure and function are reflected in the transcriptomic profile (Fig. 7). For example, the changes in LV transcriptome observed at 530 days in WD-fed male mice may

suggest an adaptive/compensatory response to the development of systolic dysfunction.

Transcriptomic changes in metabolic and cardiac remodeling mediators in male WD-fed mice

Metabolic syndrome plays a critical role in the development of CVD. Our study observed a notable enrichment of genes associated with insulin resistance and glucagon signaling in 530-day WD-fed male mice. Evidence of insulin resistance is indicated by the increased expression of key genes, such as *Insr*, *Akt3*, and *Pik3ca*, which have previously been shown to be associated with cardiac dysfunction and dilated cardiomyopathy [38–40]. Interestingly, insulin resistance has been linked to mitochondrial dysfunction, which is associated with endothelial function and cardiovascular diseases [41]. Insulin resistance is a well-documented contributor to various metabolic disorders, including type 2 diabetes and cardiovascular diseases. Mitochondria play a key role in energy production and exhibit impaired functionality in the presence of insulin resistance, characterized by alterations in mitochondrial oxidative capacity and decreased efficiency in ATP production. Furthermore, insulin resistance has been associated with changes in the expression of genes involved in mitochondrial function. Decreased expression of the *Agt* and *Cpt1b* genes observed in our study may contribute to mitochondrial dysfunction by impairing oxidative metabolism and fatty acid β -oxidation, resulting in an energy deficit in the heart [42, 43]. These changes can result in altered mitochondrial dynamics, including decreased biogenesis and increased degradation, which contribute significantly to the metabolic complications observed in insulin-resistant conditions. Glucagon has been shown to induce gluconeogenesis by activating the cAMP response element-binding protein (CREB) transcription factor and the cAMP \rightarrow EPAC2 \rightarrow p38 α \rightarrow FoxO1 signaling pathways in the murine heart [44]. In our study, we observed a notable enrichment of genes associated with the glucagon signaling pathway in 530-day WD-fed male mice. Specifically, there was a decrease in the expression of genes encoding adenylate cyclase (*Adcy3*, *Adcy4*), p38 α (*Mapk14*), key enzymes involved in glycogen metabolism (*Gys1* and *Pygm*), and gluconeogenesis (*Pkm* and *Pfkl*). Enrichment of genes involved in the glucagon signaling and insulin resistance pathways in our study could be linked to decreased availability in energy to fuel myocyte structural and functional capacitance. Adenylate cyclases serve as a link between glucagon signaling and fatty acid (FA) metabolism. Interestingly, cardiac-specific deletion of glucagon receptor was associated with inhibition of fatty acid oxidation in wild-type mouse hearts [45]. Moreover, under conditions of high insulin levels and low glucagon levels, the production of ketones from

fatty acids is reduced [46]. Ketone bodies are an efficient energy source for the failing heart to alleviate energy starvation in cardiomyocytes. Beyond their role as fuel, ketone bodies have been shown to mitigate key pathological processes in heart failure, including inflammation, oxidative stress, and cardiac remodeling [47]. Increasing evidence suggests that ketone bodies may play a protective role in heart failure [47]. These findings support the exploration of ketone-based therapies as a novel strategy to refuel and repair the failing heart.

FA is utilized for energy by transport across the cardiomyocyte mitochondrial membrane via carnitine palmitoyltransferase 1 (*Cpt1b*), which acts as the primary bottleneck in FA oxidation [38, 48]. Additionally, FAs can be esterified into triglycerides, with intermediate production of lysophosphatidic acid (LPA), phosphatidic acid (PA), and diacylglycerol (DAG) [49]. The decreased expression levels of *Cpt1b*, as well as genes encoding enzymes involved in the conversion of LPA to DAG (*Agpat3*, *Plpp1*, *Plpp3*, *Dgkq*) observed in our study may be associated with altered FA metabolism in LV tissue as a consequence of the WD in 530 days male mice group. We also observed that the majority of deregulated pathways in LV of 530 days WD-fed male mice are linked to an upregulation of *Pik3ca*, *Akt3*, *Ampk*, and *Prkg1*, which are hub genes known to play an important role in insulin resistance, cGMP-PKG, glucagon signaling pathways [50]. Overall, these results provide evidence that WT diet primarily may induce metabolic dysregulation in cardiac tissue of male mice by 530 days of age which may have long-term functional consequences. Targeting these pathways presents significant clinical implications for treating heart failure [51–53]. By addressing the dysregulation of these pathways, therapeutic strategies could be developed to improve insulin sensitivity and metabolic function in patients with heart failure, particularly those with a history of high-fat diets. Our observations provide additional knowledge on the interplay between dietary habits and cardiovascular health, emphasizing the importance of dietary modifications as a potential therapeutic avenue.

Transcriptomic changes of genes involved in cardiomyopathies in male WD-fed mice

Our analysis showed an enrichment of DEGs in KEGG pathways associated with dilated cardiomyopathy (DCM) and hypertrophic cardiomyopathy in 530-day-old WD-fed male mice. Enriched DEGs are primarily involved in calcium homeostasis (*Cacna1h*, *Cacnb2*, *Vdac2*, *Dhpr*), cardiac muscle structure and contraction (*Ttn*, *Myh6*, *Myh7b*, *Actg1*, *Dmd*), alterations in cell–cell (*Pkp2*) and cell–extracellular matrix (*Itga1*, *Itga3*, *Itga4*, *Itga7*, *Itgav*) adhesion. Calcium homeostasis is vital in maintaining cardiac function [54, 55]. Our transcriptomic analysis

revealed decreased expression of mRNAs encoding T- and L-type voltage-gated calcium channels (*Cacna1h* and *Cacnb2*, respectively) and mitochondrial voltage-dependent anion channels (*Vdac2*). The downregulation of calcium channels observed in our study suggests a potential mechanism leading to impaired calcium homeostasis in cardiomyocytes, thereby affecting contractility and overall cardiac performance [54–56]. Moreover, our study revealed the altered expression of the Ca²⁺/calmodulin-dependent protein kinase (CaMKII) encoding gene (*Camk2b*), which is a regulator of cardiac excitation–contraction coupling and calcium homeostasis in cardiomyocytes [57]. CaMKII phosphorylates the epigenetic regulator protein histone deacetylase 4 (HDAC4), which interacts with MEF2 transcription factor (*Mef2c*) and 14-3-3 chaperone protein (*Ywhae*) [58, 59] found downregulated in the LV tissue of 530 days WD-fed male mice. Mef2 is involved in various hypertrophic pathways and contributes to cardiac remodeling during heart failure [59]. As for the 14-3-3 chaperone protein, it orchestrates cardiac metabolic homeostasis and proteostasis by coordinating protein synthesis and quality control in ribosomes and mitochondria in the LV of mouse hearts [60]. Dysregulation of these proteins identified in our study at 540 days of age could elevate the risk of developing contractile dysfunction or inappropriate remodeling in WD-fed male mice later in life. Furthermore, changes in downstream effector genes were also observed, including decreased levels of transcription factor GATA-4 and its associated targets myosin heavy chain genes (*Myh6*, *Myh7*), which are involved in ventricular hypertrophic remodeling and whose dysfunction is often linked to the development of cardiomyopathies [61–66]. Interestingly, there was also a significant upregulation of titin in LV of WD 530 days male mice. Alterations in titin levels and phosphorylation of titin by CaMKII have been shown to be involved in myocardial passive stiffness and stress-sensitive signaling [67], and changes in transcript levels of these proteins found in our study may have contributed to impaired systolic function observed in our study by 750 days of age.

We also found dysregulation of genes encoding cytoskeleton proteins (downregulated: γ -actin; up-regulated: *Dmd*, *Pkp2*) and signaling component integrin α subunit (*Itga1*, *Itga3*, *Itga4*, *Itga7*, *Itgav*). Integrin α plays a pivotal role in initiating both inside-out and outside-in signaling pathways [68, 69], and has been implicated in several CVDs such as atherosclerosis, cardiac fibrosis, hypertension, and arrhythmias [70–73]. Additionally, studies have demonstrated the significant involvement of α V integrins in the progression of cardiac fibrosis [74, 75].

At a later time point (750 days), WD-fed male mice exhibit continued upregulation of the PI3K key regulator gene (*Pik3ip1*) expression in LV tissue. Several genes

involved in various lipid, xenobiotic, amino acid, and glutathione metabolic pathways display increased mRNA levels (*Adh1*, *Cys1*, *Fmo2*, *Glul*, *Mtmr14*, *Gstt2*, *Efr3b*). Myotubularin-related protein 14 (MTMR14) functions as a phosphoinositide phosphatase and has been shown to suppress cardiac hypertrophy by inhibiting the Akt pathway [76]. Glutamine synthetase (or glutamate-ammonia ligase, GLUL) and glutathione S-transferase theta 2 are enzymes crucial for cellular redox homeostasis [77, 78]. While the *GLUL* gene was recently proposed as a potential biomarker for atrial fibrillation and heart failure in humans [79], the role of *Gstt2* remains widely unknown. The altered expression of genes related to metabolic activity observed in LV tissue of 750 days WD-fed male mice may substantiate significant decreases in cardiac function manifested as a significant reduction in LVEF and LVFS at 750 days.

Transcriptomic changes in circadian rhythm and cell transport genes in female WD-fed mice

WD-fed female mice at 530 days exhibited the most distinctive set of DEGs. Notably, this group displays an abundance of DEGs related to the regulation of circadian rhythm (*Dbp*, *Arntl*, *Bhlhe41*). Studies on mouse models lacking clock genes have revealed that the circadian rhythm genes influence the regulation of up to 10% of the cardiac transcriptome [80] associated with preload, contractility, and rate [81]. The involvement of circadian rhythm regulators in the pathogenesis of cardiac arrhythmias, myocardial infarction, cardiomyopathy, and heart failure has been extensively documented [82–84]. Circadian genes play a key role in regulating inflammatory processes and lipid metabolism, and their dysregulation can lead to the development of atherosclerosis and thrombosis [85]. Recent studies have emphasized the significance of peripheral circadian clock dysregulation in controlling local tissue function [86]. In this context, our findings highlight the interplay between the dysregulation of metabolic and hormonal pathways and changes in circadian gene expression in heart tissue, suggesting that circadian genes may serve as promising therapeutic targets for preventing and treating cardiovascular diseases.

We also observed significant dysregulation of the metalloproteinase 19 (adamalysin 19) gene (*Adam19*) transcripts. This gene is pivotal in cardiovascular morphogenesis, and its expression may be influenced by cell density or cell–cell interactions [87, 88]. At 530 days of age, transcripts of genes involved in metabolism were also found to be differentially regulated, including *Mthfr*, which encodes methylenetetrahydrofolate reductase, which was significantly up regulated. This enzyme regulates cellular homeostasis and the balance between methionine and homocysteine to prevent cellular dysfunction [89]. Several genetic variants in the *Mthfr* gene

have been reported to be associated with an increased risk of CVDs and cardiovascular complications [90].

At 640 days, WD-fed female mice exhibit changes in the expression of genes known to be associated with cardiac function and energy metabolism. Notably, more than one-fourth of the DEGs encode membrane channels responsible for transporting amino acids (*Slc7a6*), calcium (*Cacna1a*) and magnesium (*Slc41a3*), water, and glycerol molecules (*Aqp7*). The *Slc7a6* gene belongs to the *Slc7* family of heterodimeric amino acid transporters, which play a crucial role in vascular function, their association with CVD risk, and their involvement in inflammation and autoimmunity [91–93]. The *Cacna1a* and *Slc41a3* genes participate in Ca^{2+} and Mg^{2+} homeostasis, which can have an impact on cardiac function and have diverse effects on vascular tone, peripheral vascular resistance, and myocardial metabolism [94, 95]. Yet another channel-encoding gene identified in our study as up-regulated in LV tissue is aquaglyceroporin *Aqp7*, which is involved in cardiac energy production [96]. The upregulation of *Aqp7* gene in skeletal muscle tissue has been reported to be involved in increased lipid accumulation in obese mice and contributes to insulin resistance in skeletal muscle and cardiac tissue [97]. Interestingly, we also saw altered expression of angiotensin-like protein 2 transcript (*Angptl2*) in LV tissue of WD-fed female mice, which is a proinflammatory mediator involved in the acceleration of the development of insulin resistance, endothelial dysfunction, atherosclerosis, and remodeling in murine models [98–101]. *Angptl2* has also been suggested to be a novel risk factor for the development of CVD that may be mediated by metabolic disorders and chronic inflammation [102]. Decreased expression of *Angptl2* observed in the LV tissue of WD-fed female mice might have a protective effect. In contrast, male mice exhibit increased expression of another angiotensin-like protein, *Angptl7*, which is a known regulator of extracellular matrix remodeling and inflammatory responses [103]. Notably, elevated levels of ANGPTL7 have been associated with increased mortality in patients with acute heart failure [103]. Angiotensin-like (ANGPTL) proteins, particularly ANGPTL3, ANGPTL4, and ANGPTL8, have emerged as critical regulators of lipid metabolism and potential therapeutic targets for cardiovascular diseases [104]. These results highlight the potential of targeting angiotensin-like proteins as a novel strategy for developing treatments for cardiovascular diseases. Our findings may suggest that WD-fed female mice may be more prone to develop insulin resistance and metabolic dysfunction through alternate pathways involving altered channels, junctional proteins, and inflammation rather than more traditional pathways observed in WD-fed male mice.

In female mice at 640 days of age, we also saw the downregulation of transcripts of structural and hemostatic proteins, including tetraspanin 4 (*Tspan4*), a member of membrane proteins, whose abnormal expression has been implicated in the progression of atherosclerosis in an inducible myocardial infarction mouse model [105]. Additionally, we observed the decreased expression of the Rho-related BTB domain-containing 1 (*Rhobtb1*) gene, which was shown to be involved in the regulation of cardiomyocyte proliferation through the modulation of miR-31a-5p in mice [106]. It has also been shown to be involved in the regulation of blood pressure in genome-wide complex trait analysis and was demonstrated to reverse arterial stiffness in angiotensin II-induced hypertension by promoting actin depolymerization [107]. Finally, we found upregulation of the gene encoding von Willebrand factor A domain containing 3A (*Vwa3a*), which is involved in blood clotting, platelet plug formation, hemostasis, and thrombosis [108] and is reported to be associated with the risk of CVD [109]. Overall, the significant structural alterations observed in the hearts of WD-fed female mice at 640 days were reflected in the transcriptome landscape of the LV tissue. This was evident by the dysregulation of several key regulatory genes involved in cardiac energy metabolism and remodeling.

Despite these insights, our study encountered limitations. We were unable to collect tissue from female mice at 750 days of age, as they began to die earlier than the males. Additionally, direct correlations between echocardiography and transcriptomics data could not be made, as the data for both studies may not have been paired from the same animal. Furthermore, we used the C57BL/6 J strain in our study, which has a deletion in *Nnt* gene, potentially affecting the heart's oxidative stress response and overall metabolic profile under high-fat dietary conditions. This strain is widely used in the field of obesity and diabetes research [110]. However, future research should expand to include other mouse strains and experimental animals, and investigations are needed to explore how the transcriptomic changes observed in our study translate to the proteomic level in cardiac tissue.

Conclusions

In summary, our study demonstrated that WD causes long-term echocardiographic functional and structural changes in the heart and induces transcriptome perturbations. Specifically, our results show that—(i) WD led to the development of HFrEF-like phenotype (systolic dysfunction) in male mice at later life stages, evidenced by decreased LVEF and LVFS, however, without detectable structural changes; (ii) in contrast, female mice WD led to the heart failure resembling HFpEF-like phenotype with detectable structural changes evidenced

by increases in LVEDd, LVIDd, LV mass and significant decrease in DWS and RWT, suggesting possible development of diastolic stiffness and dilated LV remodeling. These sex-associated pathophysiological changes were reflected in the LV tissue transcriptomic profiles of male and female mice, specifically—(i) transcriptome analysis of WD-fed male mice at 530 days of age revealed the highest number of DEGs enriched for pathways related to endocrine regulation (glucagon signaling and insulin resistance), signal transduction (cGMP-PKG), and cardiomyopathies; (ii) At 750 days in WD-fed male mice, there was continued upregulation of *Pik3ip1* and dysregulation of genes involved in lipid, glucagon, and glutathione metabolism; (iii) transcriptome analysis of LV tissue in WD-fed female mice at 530 days of age identified a distinct set of DEGs, prominently featuring genes associated with circadian rhythm regulation; (iv) at 640 days in WD-fed female mice dysregulation of genes involved in cardiac energy metabolism and remodeling was observed.

It is worth noting that the changes observed in our study persisted even after a significant amount of time following the switch to a normal diet, suggesting that early exposure to WD may have persistent effects on cardiac physiology irrespective of switching back to a “healthy diet”. While this highlights the importance of discussing the impact of diet and risk reduction at the early stages of life, this does not mitigate the importance of adopting a “heart healthy” diet as it continues to be a critical factor in mitigating disease morbidity and mortality. Another important finding is the observed sex-associated long-term effects in cardiac tissue responses. In males, it is linked to metabolic dysregulation (insulin resistance, glucagon signaling), while in females, cardiac structural changes are associated with WD-induced alterations in circadian cycle genes. This highlights the importance of considering sex-dependent factors driving cardiac disease pathophysiology, as this may provide more targeted approaches to preventing and treating CVD.

Abbreviations

WD	Western diet
ND	Normal diet
LV	Left ventricle
CVD	Cardiovascular disease
DEG	Differentially expressed genes
HFrEF	Heart failure with reduced ejection fraction
HFpEF	Heart failure with preserved ejection fraction
ECHO	Echocardiography
LVEF	Left ventricular ejection fraction
LVFS	Left ventricular fractional shortening
ESV	End-systolic volume
EDV	End-diastolic volume
LVEDd	Left ventricular end-diastolic diameter
LVESD	Left ventricular end-systolic diameter
LVPWd	Left ventricular posterior wall thickness at end-diastole
LVPWs	Left ventricular posterior wall thickness at end-systole
IVSd	Interventricular septal thickness in diastole
LVIDd	Left ventricular internal diameter in diastole

LVIDs	Left ventricular internal diameter in systole
DWS	Diastolic wall stress
AMPK	AMP-activated protein kinase
DCM	Dilated cardiomyopathy
ARVC	Arrhythmogenic right ventricular cardiomyopathy
cGMP-PKG	Cyclic guanosine monophosphate-protein kinase G
CREB	CAMP response element-binding protein
FA	Fatty acid
LPA	Lysophosphatidic acid
PA	Phosphatidic acid
DAG	Diacylglycerol
GO	Gene ontology
FDR	False discovery rate
FC	Fold change
ApoE	Apolipoprotein E
LDLR	Low-density lipoprotein receptor
WT	Wild-type

Supplementary Information

The online version contains supplementary material available at <https://doi.org/10.1186/s12933-024-02565-9>.

Supplemental file 1: Detailed report on the number of animals for treatment groups, sequencing data quality per sample, noted causes of death in male and female mice.

Supplemental file 2: Summary of up- and downregulated genes across all comparison groups (normal diet (ND) vs western diet (WD) for 530 days females; ND vs WD for 750 days males; ND vs WD for 640 days females; ND vs WD for 530 days males).

Supplemental file 3: Up- and downregulated long non-coding RNA and associated protein-coding differentially expressed genes in normal diet (ND) vs western diet (WD) for 530 days male mice comparison group.

Acknowledgements

The authors would like to acknowledge the support of Peter Guida, MaryAnn Petry, and their staff on the NASA support team at the Biology Department and BLAF animal facility at Brookhaven National Laboratory for their help with our longitudinal mouse lifetime studies.

Author contributions

Conceptualization: D.A.G., A.A.; methodology: S.H., S.D., G.K., T.S., A.B., A.S., and V.N.S.G.; software: S.H., S.S., L.H. and S.D.; validation: A.B., M.B. and M.K.K.; formal analysis: A.B., M.B., S.H., T.S., A.S., A.R. and G.K.; investigation: A.B., M.B., M.K.K., S.Z., R.Z., S.H., S.D., A.S., A.A., V.N.S.G. and D.A.G.; resources: V.N.S.G., L.H. and D.A.G.; data curation: A.B., A.A. and D.A.G.; original draft preparation: A.S., A.B., A.A. and D.A.G.; reviewing and editing: A.S., A.B., S.H., S.D., G.K., T.S., A.R., V.N.S.G., R.Z., A.A. and D.A.G.; visualization: S.H., S.D., T.S., G.K., A.S., A.A., and D.A.G.; supervision: A.A. and D.A.G.; project administration: A.A. and D.A.G.; funding acquisition: A.A. and D.A.G. All authors have read and agreed to the published version of the manuscript.

Funding

This work was funded by the NASA Human Research Program, grant No: 80NSSC19K1079 (formerly, 80NSSC18K0921) and grant No: 80NSSC21K0549 (PI - Kenneth Walsh, DAG - subcontract) to D.A.G. and the ADVANCE Research Grant provided by the Foundation for Armenian Science and Technology. This study was also supported by NIH/NHLBI grants 1K01HL159038-01A1 and 5R25HL146166, and the American Heart Association grant 24CDA1269532 (to M.B.), and NIH/NHLBI R01HL158998-01A1 and R01HL173203-01, NIH/NCATS R03TR004673 to L.H., and American Lung Association Innovation Award 1056600, and American Heart Association Award to L.H. The funders had no role in the data collection and analysis, the decision to publish, or the manuscript preparation.

Availability of data and materials

All data generated or analyzed during this study are included in this published article and its Supplementary Materials. Sequencing raw data is available at the Gene Expression Omnibus (GEO) under the accession number GSE272168.

Declarations

Ethics approval and consent to participate

All animal procedures were performed following the standards of the Guide for the Care and Use of Laboratory Animals for the National Institutes of Health and approved by the Animal Care and Use Committees at Brookhaven National Laboratory (BNL) (Upton, NY) (BNL IACUC Protocol #502) and the Icahn School of Medicine at Mount Sinai (NY, NY) (ISMMS IACUC Protocol #2019-0017).

Consent for publication

Not applicable.

Competing interests

The authors declare no competing interests.

Author details

¹Institute of Molecular Biology, National Academy of Science of Republic of Armenia, 7 Ezras Hasratyan Street, 0014 Yerevan, Armenia

²Cardiovascular Research Institute, Icahn School of Medicine at Mount Sinai, 1470 Madison Ave, s7-119, New York, NY, USA

³Department of Cell Biology, Yale School of Medicine, New Haven, CT, USA

⁴Department of Cell Biology and Anatomy and Physiology, New York Medical College, Valhalla, NY, USA

⁵Department of Pharmacological Sciences, Icahn School of Medicine at Mount Sinai, New York, NY, USA

⁶Aging + Cardiovascular Discovery Center, Department of Cardiovascular Sciences Lewis Katz School of Medicine, Temple University, Philadelphia, USA

Received: 3 December 2024 / Accepted: 24 December 2024

Published online: 28 December 2024

References

1. Tsao CW, Aday AW, Almarazooq ZI, Anderson CAM, Arora P, Avery CL, Baker-Smith CM, Beaton AZ, Boehme AK, Buxton AE, et al. Heart disease and stroke statistics-2023 update: a report from the American Heart Association. *Circulation*. 2023;147(8):e93–621.
2. Zhao Y, Li D, Huang T. Associations of dietary flavonoids and subclasses with total and cardiovascular mortality among 369,827 older people: the NIH-AARP Diet and Health Study. *Atherosclerosis*. 2023;365:1–8.
3. Said MA, Verweij N, van der Harst P. Associations of combined genetic and lifestyle risks with incident cardiovascular disease and diabetes in the UK biobank study. *JAMA Cardiol*. 2018;3(8):693–702.
4. Pazoki R, Dehghan A, Evangelou E, Warren H, Gao H, Caulfield M, Elliott P, Tzoulaki I. Genetic predisposition to high blood pressure and lifestyle factors: associations with midlife blood pressure levels and cardiovascular events. *Circulation*. 2018;137(7):653–61.
5. Charbonneau B, O'Connor HM, Wang AH, Liebow M, Thompson CA, Fredericksen ZS, Macon WR, Slager SL, Call TG, Habermann TM, et al. Trans fatty acid intake is associated with increased risk and n3 fatty acid intake with reduced risk of non-Hodgkin lymphoma. *J Nutr*. 2013;143(5):672–81.
6. Clemente-Suarez VJ, Beltran-Velasco AI, Redondo-Florez L, Martin-Rodriguez A, Tornero-Aguilera JF: Global Impacts of Western Diet and Its Effects on Metabolism and Health: A Narrative Review. *Nutrients* 2023, 15(12).
7. Malesza IJ, Malesza M, Walkowiak J, Mussin N, Walkowiak D, Aringazina R, Bartkowiak-Wieczorek J, Madry E. High-fat, western-style diet, systemic inflammation, and gut microbiota: a narrative review. *Cells*. 2021;10(11):3164.
8. Wieckowska-Gacek A, Mietelska-Porowska A, Wydrych M, Wojda U. Western diet as a trigger of Alzheimer's disease: from metabolic syndrome and systemic inflammation to neuroinflammation and neurodegeneration. *Ageing Res Rev*. 2021;70: 101397.
9. Oikonomou E, Psaltopoulou T, Georgiopoulos G, Siasos G, Kokkou E, Antonopoulos A, Vogiatzi G, Tsalamandris S, Gennimata V, Papanikolaou A, et al. Western dietary pattern is associated with severe coronary artery disease. *Angiology*. 2018;69(4):339–46.
10. Santulli G, Pascale V, Finelli R, Visco V, Giannotti R, Massari A, Morisco C, Ciccarelli M, Illario M, Iaccarino G, et al. We are what we eat: impact of food from short supply chain on metabolic syndrome. *J Clin Med*. 2019;8(12):2061.
11. Maurya SK, Carley AN, Maurya CK, Lewandowski ED. Western diet causes heart failure with reduced ejection fraction and metabolic shifts after diastolic dysfunction and novel cardiac lipid derangements. *JACC Basic Transl Sci*. 2023;8(4):422–35.
12. Liu IF, Lin TC, Wang SC, Yen CH, Li CY, Kuo HF, Hsieh CC, Chang CY, Chang CR, Chen YH, et al. Long-term administration of Western diet induced metabolic syndrome in mice and causes cardiac microvascular dysfunction, cardiomyocyte mitochondrial damage, and cardiac remodeling involving caveolae and caveolin-1 expression. *Biol Direct*. 2023;18(1):9.
13. Christ A, Lauterbach M, Latz E. Western diet and the immune system: an inflammatory connection. *Immunity*. 2019;51(5):794–811.
14. Pavillard LE, Marin-Aguilar F, Bullon P, Cordero MD. Cardiovascular diseases, NLRP3 inflammasome, and western dietary patterns. *Pharmacol Res*. 2018;131:44–50.
15. Ye S, Matthan NR, Lamon-Fava S, Aguilar GS, Turner JR, Walker ME, Chai Z, Lakshman S, Urban JF Jr, Lichtenstein AH. Western and heart healthy dietary patterns differentially affect the expression of genes associated with lipid metabolism, interferon signaling and inflammation in the jejunum of Ossabaw pigs. *J Nutr Biochem*. 2021;90: 108577.
16. Gambardella J, Santulli G. Integrating diet and inflammation to calculate cardiovascular risk. *Atherosclerosis*. 2016;253:258–61.
17. Sharif S, Van der Graaf Y, Cramer MJ, Kapelle LJ, de Borst GJ, Visseren FLJ, Westerink J. group Ss: low-grade inflammation as a risk factor for cardiovascular events and all-cause mortality in patients with type 2 diabetes. *Cardiovasc Diabetol*. 2021;20(1):220.
18. Norton CE, Jacobsen NL, Sinkler SY, Manrique-Acevedo C, Segal SS. Female sex and Western-style diet protect mouse resistance arteries during acute oxidative stress. *Am J Physiol Cell Physiol*. 2020;318(3):C627–39.
19. Talley S, Bonomo R, Gavini C, Hatahet J, Gornick E, Cook T, Chun BJ, Kekenus-Huskey P, Aubert G, Campbell E, et al. Monitoring of inflammation using novel biosensor mouse model reveals tissue- and sex-specific responses to Western diet. *Dis Model Mech*. 2022. <https://doi.org/10.1242/dmm.049313>.
20. Shafer CC, Di Lucente J, Mendiola UR, Maezawa I, Jin LW, Neumann EK. Effects of sex and western diet on spatial lipidomic profiles for the hippocampus, cortex, and corpus callosum in mice using MALDI MSI. *J Am Soc Mass Spectrom*. 2024;35:2554–63.
21. Hunter I, Soler A, Joseph G, Hutcheson B, Bradford C, Zhang FF, Potter B, Proctor S, Rocic P. Cardiovascular function in male and female JCR:LA-cp rats: effect of high-fat/high-sucrose diet. *Am J Physiol Heart Circ Physiol*. 2017;312(4):H742–51.
22. Colom B, Oliver J, Roca P, Garcia-Palmer FJ. Caloric restriction and gender modulate cardiac muscle mitochondrial H2O2 production and oxidative damage. *Cardiovasc Res*. 2007;74(3):456–65.
23. Schneider J, Kury S, Beker D, Sauve Y, Lemieux H. Cardiovascular sexual dimorphism in a diet-induced type 2 diabetes rodent model, the Nile rat (*Arvicanthis niloticus*). *PLoS ONE*. 2018;13(12): e0208987.
24. Leening MJ, Ferket BS, Steyerberg EW, Kavousi M, Deckers JW, Nieboer D, Heeringa J, Portegies ML, Hofman A, Ikram MA, et al. Sex differences in lifetime risk and first manifestation of cardiovascular disease: prospective population based cohort study. *BMJ*. 2014;349: g5992.
25. Niiranen TJ, Lyass A, Larson MG, Hamburg NM, Benjamin EJ, Mitchell GF, Vasan RS. Prevalence, correlates, and prognosis of healthy vascular aging in a western community-dwelling cohort: the framingham heart study. *Hypertension*. 2017;70(2):267–74.
26. Zhou Y, Wan X, Seidel K, Zhang M, Goodman JB, Seta F, Hamburg N, Han J. Aging and hypercholesterolemia differentially affect the unfolded protein response in the vasculature of ApoE(-/-) mice. *J Am Heart Assoc*. 2021;10(18): e020441.
27. Flurkey K, et al. The mouse in aging research. In: Fox JG, et al., editors. *The mouse in biomedical research*. American college laboratory animal medicine. 2nd ed. Burlington: Elsevier; 2007. p. 637–72.
28. Dobin A, Davis CA, Schlesinger F, Drenkow J, Zaleski C, Jha S, Batut P, Chaisson M, Gingeras TR. STAR: ultrafast universal RNA-seq aligner. *Bioinformatics*. 2013;29(1):15–21.
29. Love MI, Huber W, Anders S. Moderated estimation of fold change and dispersion for RNA-seq data with DESeq2. *Genome Biol*. 2014;15(12):550.
30. Kuleshov MV, Jones MR, Rouillard AD, Fernandez NF, Duan Q, Wang Z, Koplev S, Jenkins SL, Jagodnik KM, Lachmann A, et al. Enrichr: a comprehensive gene set enrichment analysis web server 2016 update. *Nucleic Acids Res*. 2016;44(W1):W90–97.
31. Ngo GHP, Grimstead JW, Baird DM. UPF1 promotes the formation of R loops to stimulate DNA double-strand break repair. *Nat Commun*. 2021;12(1):3849.

32. Hou J, Zhang G, Wang X, Wang Y, Wang K. Functions and mechanisms of lncRNA MALAT1 in cancer chemotherapy resistance. *Biomark Res.* 2023;11(1):23.
33. Chen BL, Wang HM, Lin XS, Zeng YM. UPF1: a potential biomarker in human cancers. *Front Biosci (Landmark Ed).* 2021;26(5):76–84.
34. Fang CX, Dong F, Thomas DP, Ma H, He L, Ren J. Hypertrophic cardiomyopathy in high-fat diet-induced obesity: role of suppression of forkhead transcription factor and atrophy gene transcription. *Am J Physiol Heart Circ Physiol.* 2008;295(3):H1206–15.
35. Arias-Chavez DJ, Mailloux-Salinas P, Aparicio JL, Bravo G, Gomez-Viquez NL. Combined fructose and sucrose consumption from an early age aggravates cardiac oxidative damage and causes a dilated cardiomyopathy in SHR rats. *J Clin Biochem Nutr.* 2023;73(3):205–13.
36. Hasegawa Y, Chen SY, Sheng L, Jena PK, Kalanetra KM, Mills DA, Wan YY, Slupsky CM. Long-term effects of western diet consumption in male and female mice. *Sci Rep.* 2020;10(1):14686.
37. Lord MN, Heo JW, Schifino AG, Hoffman JR, Donohue KN, Call JA, Noble EE. Sexually dimorphic effects of a western diet on brain mitochondrial bioenergetics and neurocognitive function. *Nutrients.* 2021;13(12):4222.
38. Abel ED, O'Shea KM, Ramasamy R. Insulin resistance: metabolic mechanisms and consequences in the heart. *Arterioscler Thromb Vasc Biol.* 2012;32(9):2068–76.
39. Qi Y, Xu Z, Zhu Q, Thomas C, Kumar R, Feng H, Dostal DE, White MF, Baker KM, Guo S. Myocardial loss of IRS1 and IRS2 causes heart failure and is controlled by p38alpha MAPK during insulin resistance. *Diabetes.* 2013;62(11):3887–900.
40. Yan H, Yang W, Zhou F, Pan Q, Allred C, Allred C, Sun Y, Threadgill D, Dostal D, Tong C, et al. Estrogen protects cardiac function and energy metabolism in dilated cardiomyopathy induced by loss of cardiac IRS1 and IRS2. *Circ Heart Fail.* 2022;15(6): e008758.
41. Mone P, Morgante M, Pansini A, Jankauskas SS, Rizzo M, Lombardi A, Frullone S, Santulli G. Effects of insulin resistance on mitochondrial (dys)function. *Atherosclerosis.* 2022;341:52–4.
42. Dai DF, Johnson SC, Villarín JJ, Chin MT, Nieves-Cintrón M, Chen T, Marcinek DJ, Dorn GW 2nd, Kang YJ, Prolla TA, et al. Mitochondrial oxidative stress mediates angiotensin II-induced cardiac hypertrophy and Galphaq overexpression-induced heart failure. *Circ Res.* 2011;108(7):837–46.
43. He L, Kim T, Long Q, Liu J, Wang P, Zhou Y, Ding Y, Prasain J, Wood PA, Yang Q. Carnitine palmitoyltransferase-1b deficiency aggravates pressure overload-induced cardiac hypertrophy caused by lipotoxicity. *Circulation.* 2012;126(14):1705–16.
44. Neumann J, Hofmann B, Dhein S, Gergs U. Glucagon and its receptors in the mammalian heart. *Int J Mol Sci.* 2023;24(16):12829.
45. Karwi QG, Zhang L, Wagg CS, Wang W, Ghandi M, Thai D, Yan H, Ussher JR, Oudit GY, Lopaschuk GD. Targeting the glucagon receptor improves cardiac function and enhances insulin sensitivity following a myocardial infarction. *Cardiovasc Diabetol.* 2019;18(1):1.
46. Capozzi ME, Coch RW, Koech J, Astapova II, Wait JB, Encisco SE, Douros JD, El K, Finan B, Sloop KW, et al. The limited role of glucagon for ketogenesis during fasting or in response to SGLT2 inhibition. *Diabetes.* 2020;69(5):882–92.
47. Yurista SR, Nguyen CT, Rosenzweig A, de Boer RA, Westenbrink BD. Ketone bodies for the failing heart: fuels that can fix the engine? *Trends Endocrinol Metab.* 2021;32(10):814–26.
48. Actis Dato V, Lange S, Cho Y. Metabolic flexibility of the heart: the role of fatty acid metabolism in health, heart failure, and cardiometabolic diseases. *Int J Mol Sci.* 2024;25(2):1211.
49. Prentki M, Madiraju SR. Glycerolipid metabolism and signaling in health and disease. *Endocr Rev.* 2008;29(6):647–76.
50. Kanehisa M, Furumichi M, Sato Y, Kawashima M, Ishiguro-Watanabe M. KEGG for taxonomy-based analysis of pathways and genomes. *Nucleic Acids Res.* 2023;51(D1):D587–92.
51. Marino A, Hausenloy DJ, Andreadou I, Horman S, Bertrand L, Beauloye C. AMP-activated protein kinase: a remarkable contributor to preserve a healthy heart against ROS injury. *Free Radic Biol Med.* 2021;166:238–54.
52. Zhang Q, Wang L, Wang S, Cheng H, Xu L, Pei G, Wang Y, Fu C, Jiang Y, He C, et al. Signaling pathways and targeted therapy for myocardial infarction. *Signal Transduct Target Ther.* 2022;7(1):78.
53. Ashraf FUN, Ghouri K, Someshwar F, Kumar S, Kumar N, Kumari K, Bano S, Ahmad S, Khawar MH, Ramchandani L, et al. Insulin resistance and coronary artery disease: untangling the web of endocrine-cardiac connections. *Cureus.* 2023;15(12): e51066.
54. Eisner DA, Caldwell JL, Kistamas K, Trafford AW. Calcium and excitation-contraction coupling in the heart. *Circ Res.* 2017;121(2):181–95.
55. Sommese LM, Racioppi MF, Shen X, Orłowski A, Valverde CA, Louch WE, Vila Petroff M, Gonano LA. Discordant Ca(2+) release in cardiac myocytes: characterization and susceptibility to pharmacological RyR2 modulation. *Pflugers Arch.* 2022;474(6):625–36.
56. Rosenberg P. VDACC2 as a novel target for heart failure: Ca(2+) at the sarco-mere, mitochondria and SR. *Cell Calcium.* 2022;104: 102586.
57. Wood BM, Simon M, Galice S, Alim CC, Ferrero M, Pinna NN, Bers DM, Bossuyt J. Cardiac CaMKII activation promotes rapid translocation to its extra-dyadic targets. *J Mol Cell Cardiol.* 2018;125:18–28.
58. Kreusser MM, Backs J. Integrated mechanisms of CaMKII-dependent ventricular remodeling. *Front Pharmacol.* 2014;5:36.
59. Tobin SW, Hashemi S, Dadson K, Turdi S, Ebrahimi K, Zhao J, Sweeney G, Grigull J, McDermott JC. Heart failure and MEF2 transcriptome dynamics in response to beta-blockers. *Sci Rep.* 2017;7(1):4476.
60. Qu JH, Tarasov KV, Chakir K, Tarasova YS, Riordon DR, Lakatta EG. Proteomic landscape and deduced functions of the cardiac 14–3–3 protein interactome. *Cells.* 2022;11(21):3496.
61. Ku PM, Chen LJ, Liang JR, Cheng KC, Li YX, Cheng JT. Molecular role of GATA binding protein 4 (GATA-4) in hyperglycemia-induced reduction of cardiac contractility. *Cardiovasc Diabetol.* 2011;10:57.
62. Oka T, Xu J, Molkentin JD. Re-employment of developmental transcription factors in adult heart disease. *Semin Cell Dev Biol.* 2007;18(1):117–31.
63. Hershnkovitz T, Kurolop A, Ruhman-Shahar N, Monakier D, DeChene ET, Peretz-Amit G, Funke B, Zucker N, Hirsch R, Tan WH, et al. Clinical diversity of MYH7-related cardiomyopathies: insights into genotype-phenotype correlations. *Am J Med Genet A.* 2019;179(3):365–72.
64. Gao Y, Peng L, Zhao C. MYH7 in cardiomyopathy and skeletal muscle myopathy. *Mol Cell Biochem.* 2024;479(2):393–417.
65. Razmara E, Garshabi M. Whole-exome sequencing identifies R1279X of MYH6 gene to be associated with congenital heart disease. *BMC Cardiovasc Disord.* 2018;18(1):137.
66. Tomita-Mitchell A, Stamm KD, Mahnke DK, Kim MS, Hidestrand PM, Liang HL, Goetsch MA, Hidestrand M, Simpson P, Pelech AN, et al. Impact of MYH6 variants in hypoplastic left heart syndrome. *Physiol Genomics.* 2016;48(12):912–21.
67. LeWinter MM, Granzier HL. Cardiac titin and heart disease. *J Cardiovasc Pharmacol.* 2014;63(3):207–12.
68. Takada Y, Ye X, Simon S. The integrins. *Genome Biol.* 2007;8(5):215.
69. Seetharaman S, Etienne-Manneville S. Integrin diversity brings specificity in mechanotransduction. *Biol Cell.* 2018;110(3):49–64.
70. Xu J, Shi GP. Vascular wall extracellular matrix proteins and vascular diseases. *Biochim Biophys Acta.* 2014;1842(11):2106–19.
71. Zhou P, Yang X, Yang D, Jiang X, Wang WE, Yue R, Fang Y. Integrin-linked kinase activation prevents ventricular arrhythmias induced by ischemia/reperfusion via inhibition of connexin 43 remodeling. *J Cardiovasc Transl Res.* 2021;14(4):610–8.
72. Schinner C, Xu L, Franz H, Zimmermann A, Wanuske MT, Rathod M, Hanns P, Geier F, Pelczar P, Liang Y, et al. Defective desmosomal adhesion causes arrhythmogenic cardiomyopathy by involving an integrin-alpha6beta6/TGF-beta signaling cascade. *Circulation.* 2022;146(21):1610–26.
73. Zhang S, Zhang Q, Lu Y, Chen J, Liu J, Li Z, Xie Z. Roles of integrin in cardiovascular diseases: from basic research to clinical implications. *Int J Mol Sci.* 2024;25(7):4096.
74. Chen C, Li R, Ross RS, Manso AM. Integrins and integrin-related proteins in cardiac fibrosis. *J Mol Cell Cardiol.* 2016;93:162–74.
75. Kanaan R, Medlej-Hashim M, Jounblat R, Pilecki B, Sorensen GL. Microfibrillar-associated protein 4 in health and disease. *Matrix Biol.* 2022;111:1–25.
76. Zhang JL, Zhang DH, Li YP, Wu LM, Liang C, Yao R, Wang Z, Feng SD, Wang ZM, Zhang YZ. Myotubularin-related protein 14 suppresses cardiac hypertrophy by inhibiting Akt. *Cell Death Dis.* 2020;11(2):140.
77. Eelen G, Dubois C, Cantelmo AR, Goveia J, Bruning U, DeRan M, Jarugumilli G, van Rijssel J, Saladino G, Comitani F, et al. Role of glutamine synthetase in angiogenesis beyond glutamine synthesis. *Nature.* 2018;561(7721):63–9.
78. Song Y, Shan Z, Luo C, Kang C, Yang Y, He P, Li S, Chen L, Jiang X, Liu L. Glutathione S-transferase T1 (GSTT1) null polymorphism, smoking, and their interaction in coronary heart disease: a comprehensive meta-analysis. *Heart Lung Circ.* 2017;26(4):362–70.
79. Zhang Z, Ding J, Mi X, Lin Y, Li X, Lian J, Liu J, Qu L, Zhao B, Li X. Identification of common mechanisms and biomarkers of atrial fibrillation and heart failure based on machine learning. *ESC Heart Fail.* 2024;11:2323–33.
80. Zhang J, Chatham JC, Young ME. Circadian regulation of cardiac physiology: rhythms that keep the heart beating. *Annu Rev Physiol.* 2020;82:79–101.

81. Takeda N, Maemura K. The role of clock genes and circadian rhythm in the development of cardiovascular diseases. *Cell Mol Life Sci*. 2015;72(17):3225–34.
82. Malhan D, Relogio A. A matter of timing? The influence of circadian rhythms on cardiac physiology and disease. *Eur Heart J*. 2024;45(8):561–3.
83. Skrclec I. Circadian system microRNAs—Role in the development of cardiovascular diseases. *Adv Protein Chem Struct Biol*. 2023;137:225–67.
84. Lin J, Kuang H, Jiang J, Zhou H, Peng L, Yan X, Kuang J. Circadian rhythms in cardiovascular function: implications for cardiac diseases and therapeutic opportunities. *Med Sci Monit*. 2023;29: e942215.
85. Man AWC, Li H, Xia N. Circadian rhythm: potential therapeutic target for atherosclerosis and thrombosis. *Int J Mol Sci*. 2021;22(2):676.
86. Brown SA, Azzi A. Peripheral circadian oscillators in mammals. *Handb Exp Pharmacol*. 2013;217:45–66.
87. Qi B, Newcomer RG, Sang QX. ADAM19/adamalysin 19 structure, function, and role as a putative target in tumors and inflammatory diseases. *Curr Pharm Des*. 2009;15(20):2336–48.
88. Kurohara K, Komatsu K, Kurisaki T, Masuda A, Irie N, Asano M, Sudo K, Nabeshima Y, Iwakura Y, Sehara-Fujisawa A. Essential roles of Meltrin beta (ADAM19) in heart development. *Dev Biol*. 2004;267(1):14–28.
89. Chita DS, Tudor A, Christodorescu R, Buleu FN, Sosdean R, Deme SM, Mercea S, Pop Moldovan A, Pah AM, Docu Axelerad A, et al. MTHFR gene polymorphisms prevalence and cardiovascular risk factors involved in cardioembolic stroke type and severity. *Brain Sci*. 2020;10(8):476.
90. Raghubeer S, Matsha TE. Methylenetetrahydrofolate (MTHFR), the one-carbon cycle, and cardiovascular risks. *Nutrients*. 2021;13(12):4562.
91. Banjarnahor S, Rodionov RN, Konig J, Maas R. Transport of L-arginine related cardiovascular risk markers. *J Clin Med*. 2020;9(12):3975.
92. Kamada Y, Nagaretani H, Tamura S, Ohama T, Maruyama T, Hiraoka H, Yamashita S, Yamada A, Kiso S, Inui Y, et al. Vascular endothelial dysfunction resulting from L-arginine deficiency in a patient with lysinuric protein intolerance. *J Clin Invest*. 2001;108(5):717–24.
93. Sheng L, Luo Q, Chen L. Amino acid solute carrier transporters in inflammation and autoimmunity. *Drug Metab Dispos*. 2022;50:1228–37.
94. de Baaij JH, Arjona FJ, van den Brand M, Lavrijsen M, Lameris AL, Bindels RJ, Hoenderop JG. Identification of SLC41A3 as a novel player in magnesium homeostasis. *Sci Rep*. 2016;6:28565.
95. Negru AG, Pastorci A, Crisan S, Cismaru G, Popescu FG, Luca CT. The role of hypomagnesemia in cardiac arrhythmias: a clinical perspective. *Biomedicines*. 2022;10(10):2356.
96. Fujii M, Ota K, Bessho R. Cardioprotective effect of hyperkalemic cardioplegia in an aquaporin 7-deficient murine heart. *Gen Thorac Cardiovasc Surg*. 2020;68(6):578–84.
97. Iena FM, Lebeck J. Implications of aquaglyceroporin 7 in energy metabolism. *Int J Mol Sci*. 2018;19(1):154.
98. Sasaki Y, Ohta M, Desai D, Figueiredo JL, Whelan MC, Sugano T, Yamabi M, Yano W, Faits T, Yabusaki K, et al. Angiotensin II-like protein 2 (ANGPTL2) promotes adipose tissue macrophage and T lymphocyte accumulation and leads to insulin resistance. *PLoS ONE*. 2015;10(7): e0131176.
99. Atawia RT, Bunch KL, Toque HA, Caldwell RB, Caldwell RW. Mechanisms of obesity-induced metabolic and vascular dysfunctions. *Front Biosci (Landmark Ed)*. 2019;24(5):890–934.
100. Tian Z, Miyata K, Kadomatsu T, Horiguchi H, Fukushima H, Tohyama S, Ujihara Y, Okumura T, Yamaguchi S, Zhao J, et al. ANGPTL2 activity in cardiac pathologies accelerates heart failure by perturbing cardiac function and energy metabolism. *Nat Commun*. 2016;7:13016.
101. Tian Z, Miyata K, Morinaga J, Horiguchi H, Kadomatsu T, Endo M, Zhao J, Zhu S, Sugizaki T, Sato M, et al. Circulating ANGPTL2 levels increase in humans and mice exhibiting cardiac dysfunction. *Circ J*. 2018;82(2):437–47.
102. Hata J, Mukai N, Nagata M, Ohara T, Yoshida D, Kishimoto H, Shibata M, Hirakawa Y, Endo M, Ago T, et al. Serum angiotensin-like protein 2 is a novel risk factor for cardiovascular disease in the community: the hisayama study. *Arterioscler Thromb Vasc Biol*. 2016;36(8):1686–91.
103. Zhang C, He X, Zhao J, Cao Y, Liu J, Liang W, Zhou Y, Wang C, Xue R, Dong Y, et al. Angiotensin-like protein 7 and short-term mortality in acute heart failure. *Cardiorenal Med*. 2020;10(2):116–24.
104. Morelli MB, Chavez C, Santulli G. Angiotensin-like proteins as therapeutic targets for cardiovascular disease: focus on lipid disorders. *Expert Opin Ther Targets*. 2020;24(1):79–88.
105. Zheng Y, Lang Y, Qi B, Li T. TSPAN4 and migrasomes in atherosclerosis regression correlated to myocardial infarction and pan-cancer progression. *Cell Adh Migr*. 2023;17(1):14–9.
106. Xiao J, Liu H, Cretoiu D, Toader DO, Suciu N, Shi J, Shen S, Bei Y, Sluijter JP, Das S, et al. miR-31a-5p promotes postnatal cardiomyocyte proliferation by targeting RhoBTB1. *Exp Mol Med*. 2017;49(10): e386.
107. Fang S, Wu J, Reho JJ, Lu KT, Brozoski DT, Kumar G, Werthman AM, Silva SD Jr, Muskus Veitia PC, Wackman KK, et al. RhoBTB1 reverses established arterial stiffness in angiotensin II-induced hypertension by promoting actin depolymerization. *JCI Insight*. 2022;7(9):e158043.
108. Grunin M, Beykin G, Rahmani E, Schweiger R, Barel G, Hagbi-Levi S, Elbaz-Hayoun S, Rinsky B, Ganiel M, Carmi S, et al. Association of a variant in VWA3A with response to anti-vascular endothelial growth factor treatment in neovascular AMD. *Invest Ophthalmol Vis Sci*. 2020;61(2):48.
109. van Schie MC, de Maat MP, Isaacs A, van Duijn CM, Deckers JW, Dippel DW, Leebeek FW. Variation in the von Willebrand factor gene is associated with von Willebrand factor levels and with the risk for cardiovascular disease. *Blood*. 2011;117(4):1393–9.
110. Siersbaek MS, Ditzel N, Hejbol EK, Praestholm SM, Markussen LK, Avolio F, Li L, Lehtonen L, Hansen AK, Schroder HD, et al. C57BL/6J substrain differences in response to high-fat diet intervention. *Sci Rep*. 2020;10(1):14052.

Publisher's note

Springer Nature remains neutral with regard to jurisdictional claims in published maps and institutional affiliations.